NJC

Halogen Bonded Associates of Iodonium Salts with 18-Crown-6: Does Structural Flexibility or Structural Rigidity of the sigma-Hole Donor Provide Efficient Substrate Ligation?

Journal:	*New Journal of Chemistry*
Manuscript ID	NJ-ART-05-2024-002105.R1
Article Type:	Paper
Date Submitted by the Author:	n/a
Complete List of Authors:	Sysoeva, Alexandra; Saint Petersburg State University Novikov, Alexander; St Petersburg State University, ; ITMO University, Il'in, Mikhail; Saint Petersburg State University Institute of Chemistry, Bolotin, Dmitrii; Saint Petersburg University Institute of Chemistry,

NJC
New Journal of Chemistry
A journal for new directions in chemistry

Guidelines for Referees

Thank you very much for agreeing to review this manuscript for *New Journal of Chemistry*.

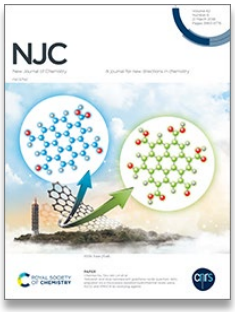

NJC (*New Journal of Chemistry*) is a broad-based primary journal encompassing all branches of chemistry and its sub-disciplines. It contains full research articles, communications, perspectives and focus articles.

Impact Factor*: **3.3** CiteScore**: **5.8**

Submissions in 2022: **6035** Publications in 2022: **2346**

For more information, visit rsc.li/metrics-explainer

*2022 Journal Citation Reports® ** CiteScore™ 2022, available from Scopus

The following manuscript has been submitted for consideration as a

PAPER

NJC offers single-anonymised peer review only.

Papers report a complete study that leads to new understanding or gives new insight into the subject under investigation. If preliminary results have been published in a communication, a subsequent full paper should include additional results that justify another publication.

We ask referees to **recommend only the most significant work** for publication in *NJC*. When making your recommendation please:

- **Comment on** the originality, importance, impact and scientific reliability of the work
- **Note that routine or incremental** work should not be recommended for publication.
- **Contact the Editor** if there is any conflict of interest, if the work has been previously published or if there is a significant part of the work which you are not able to referee with confidence.

Best regards,

Contact us

Professor Jean-François Gérard
Editor-in-Chief, *NJC*

Sally Howells-Wyllie
Executive Editor, *NJC*

Please visit our reviewer hub for further details of our processes, policies and reviewer responsibilities as well as guidance on how to review, or click the links below.

What to do when you review

Reviewer responsibilities

Process & policies

Prof. Catharine Esterhuysen
Associate Editor
New Journal of Chemistry

13th June 2024

Dear Prof. Esterhuysen,

Please find enclosed a revised version of our manuscript entitled "**Halogen Bonded Associates of Iodonium Salts with 18-Crown-6: Does Structural Flexibility or Structural Rigidity of the σ-Hole Donor Provide Efficient Substrate Ligation?**", which we would like to be considered for publication as a **Research Article** in *New Journal of Chemistry*.

Answers for the reviewer's comments are listed below. All changes to the manuscript are highlighted with yellow marker.

Reviewer #2

What was the basis of choosing CD_3CN and CD_3OD as solvents?

Due to the ionic nature diaryliodonium salts are insoluble in many common organic solvents, such as chloroform, dichloromethane, or THF. Acetonitrile and methanol has been chosen as the model solvents, in which both salts are soluble. This point was clarified in this version of the manuscript.

Page-5: "Taking into account all these experimental observations, it can be concluded that acyclic cation 1OTf exhibits higher affinity to 18-crown-6 in both chosen solvents compared to 2OTf,…)" . The text seems to be contradictory as the authors stated in line no-60 of page 3 that "Thus, in CD_3CN, the titration of 18-crown-6 with cyclic 2OTf showed points excellently fitted by the approximation curve (Figure 1, top, red line) related to K298 = 8.3(4) M^{-1}, whereas the data obtained for acyclic 1OTf was impossible to fit in the 1:1 or 1:2 approximation models due to counter-directional changes in the chemical shift of 18-crown-6 signal at low and high ratios of the iodonium salt (Figure 1, top, blue line).

In the experimental part, we mean that, in MeCN, 18-crown-6 can form 1:1 and then 1:2 associates with the acyclic salt, whereas only 1:1 associates were observed for the cyclic salt. In MeOH, the cyclic salt form too weak associates with 18-crown-6 to calculate the constant, whereas the acyclic salt forms strongly bound 1:1 associate. Considering these observations, we concluded that the acyclic salt significantly better binds the crown ether in compare to the cyclic salt. So, there is no contradictions in the text. We included small clarification to the main text (marked in yellow).

In the computation method, it is anticipated to have basis set superposition error due to different type of basis set for metal and the other atoms.
How the equilibrium geometry was assured?
What was the contribution of dispersion correction in the structure and energetics?

In the first comment, the reviewer probably means the iodine atom, and not the metal atom, because our real and model systems does not contain any metal atoms.

To assure the equilibrium geometries for all model structures, we carried out full geometry optimization procedure at the DFT level of theory with UFF pre-optimization in Avogadro program package (https://avogadro.cc/), and the Hessian matrices were calculated analytically for all DFT-

optimized model structures to prove the location of the correct minimum on the potential energy surface (no imaginary frequencies were found in all cases).

Accordingly to these three interrelated comments, we included the following clarification into the main text:

"The full geometry optimization procedure with UFF pre-optimization in Avogadro program package (https://avogadro.cc/) for all model structures was carried out at the DFT level of theory using the hybrid functional ωB97XD[30] (the addition of dispersion correction is *de facto* a standard practice in modern computational chemistry, and it was automatically internally employed in the functional ωB97XD specifically developed for these purposes) with the help of Gaussian-09[31] program package (revision C.01). The iodine is a heavy and relativistic atom and application of special basis sets and pseudopotentials for proper description of the properties of such atoms are highly desirable. By this reason, we used the quasi-relativistic MWB46 pseudopotentials, which described 46 core electrons, and the appropriate contracted basis sets for iodine atoms,[32] while the standard 6-311G* basis sets were used for all other atoms. Note that it is well known from many original articles and benchmark studies[33-36] that triple-zeta quality basis sets (including 6-311G*) are good enough and produce very small basis set superposition errors."

SMD is understood to be a continuum model and thus it needs size of the atoms and also dielectric constant of the solvent. Please include those.

Accordingly to this comment, we clarified the corresponding fragment of the main text:

"We used standard default settings for SMD model implemented in Gaussian-09 program package (revision C.01) – atomic radii: SMD-Coulomb, atomic radii for non-electrostatic terms: SMD-CDS, cavity type: VdW (van der Waals surface), cavity algorithm: GePol, solvents: acetonitrile (Eps = 35.688; Eps(inf) = 1.806874) and methanol (Eps = 32.613; Eps(inf) = 1.765709). The Hessian matrices were calculated analytically for all optimized model structures to prove the location of the correct minimum on the potential energy surface (no imaginary frequencies were found in all cases) and to estimate the thermodynamic parameters, the latter being calculated at 298 K and 1 atm."

The details of free energy calculations should be given in the main text.

The details of free energy calculations were added in the main text (see Table 1 and Computational details section).

ADDITIONAL CORRECTIONS

During the review process, we were able to prepare crystals of the **1**^{OTf}·18C6·**1**^{OTf} associate and carry out the XRD study. The corresponding data has been introduced to this version of the manuscript.

We hope that this version of the manuscript is suitable for publication in *New Journal of Chemistry* and look forward to hearing from you.

Sincerely,
Dmitrii S. Bolotin

Halogen Bonded Associates of Iodonium Salts with 18-Crown-6: Does Structural Flexibility or Structural Rigidity of the σ-Hole Donor Provide Efficient Substrate Ligation?

Alexandra A. Sysoeva,[1] Alexander S. Novikov,[1,2] Mikhail V. Il'in,[1] and Dmitrii S. Bolotin[1,*]

[1] Institute of Chemistry, Saint Petersburg State University, Universitetskaya Nab. 7/9, Saint Petersburg, 199034, Russian Federation
[2] Peoples' Friendship University of Russia (RUDN University), Miklukho-Maklaya Str. 6, 117198 Moscow, Russian Federation

* Corresponding author E-mail: d.s.bolotin@spbu.ru

Abstract

^{1}H NMR titration of 18-crown-6 with diphenyliodonium triflate and dibenziodolium triflate indicated that the acyclic iodine(III)-containing species has a higher value of the binding constant compared with that of the cyclic analogue. Formation of triple associates diphenyliodonium···18-crown-6···diphenyliodonium was observed in CD_3CN. DFT calculations and QTAIM analysis indicated that the acyclic iodonium salt forms a higher number of interactions with the crown ether compared with the cyclic cation, which results in the formation of triple associates. The formation of dibenziodolium···18-crown-6···dibenziodolium triple associates turned out energetically unfavorable, which agrees with the experimentally obtained data.

Introduction

Diaryliodonium salts play an important role in modern organic chemistry due to their useful applications in synthetic organic chemistry as reactive arylating agents and noncovalent electrophilic organocatalysts.[1] In particular, the iodonium salts effectively catalyze such important transformations as Mannich,[2] Michael,[3] and Groebke–Blackburn–Bienaymé[4-6] reactions, as well as Knoevenagel,[7] Knorr-type, [8] and Schiff condensations,[9] Ritter-type solvolysis,[10, 11] Diels-Alder reaction,[3, 11, 12] living cationic polymerization,[13] and other reactions.[14-16] Such catalytic activity is provided via the availability of a region with

positive electrostatic potential (σ-hole) on the iodine(III) center, which serves as a labile coordination vacancy capable to ligate reaction substrates. A notable catalytic activity of these σ-hole carriers is accompanied with high tolerance to water and oxygen, which positively distinguishes them from metal-containing Lewis acids.[7] These observations may indicate that the replacement of traditional hydrogen bond-donating organocatalysts,[17-20] as well as metal-containing Lewis acids, with iodonium salts can provide the next step in sustainable catalysis.

A series of experimental and theoretical studies indicates that cyclic derivatives of iodonium salts — iodolium derivatives (**Scheme 1**) — have higher catalytic activity and higher Lewis acidity than their acyclic analogues — diaryliodonium salts (**Scheme 1**),[4, 8, 21] which is explained, in particular, by higher binding constants of the former with reaction substrates leading to higher equilibrium concentration of the reactive catalyst···substrate associates.[4] This more profitable binding is provided via fixed location of the *ortho*-hydrogen atoms opposite to the iodine σ-holes leading to the formation of bifurcate halogen- and hydrogen bonding with the ligated reaction substrate.

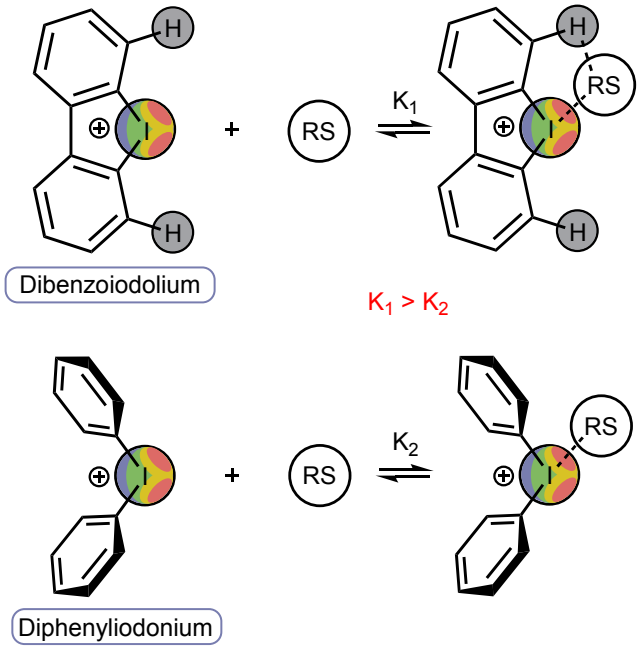

Scheme 1. Reversible association of the iodine(III)-containing cations with a reaction substrate (RS).

In this work, we decided to experimentally and theoretically examine the relative binding constants of dibenziodolium triflate and diphenyliodonium triflate with a bulky nucleophilic agent to check whether the structural flexibility of the acyclic iodonium cation leads to better binding properties compared to the cyclic congener with rigid geometry. A

better understanding of the relative activity of these two types of organocatalysts might help choose a better catalytic system in future research.

Results and Discussion

Experimental study. As model compounds, diphenyliodonium triflate **1**^{OTf} and dibenziodolium triflate **2**^{OTf} have been chosen as model iodine(III)-containing halogen bond donors. 18-Crown-6 has been chosen as a model multidentate nucleophile since its binding with some iodonium cations was studied previously in the solid-state and solution.[22-25] The binding constants have been calculated based on the ^{1}H NMR titration data obtained in acetonitrile-d_3 and methanol-d_4 utilized by us as aprotic and protic solvents, respectively, since both salts are satisfactorily soluble in these solvents (**Scheme 2**).

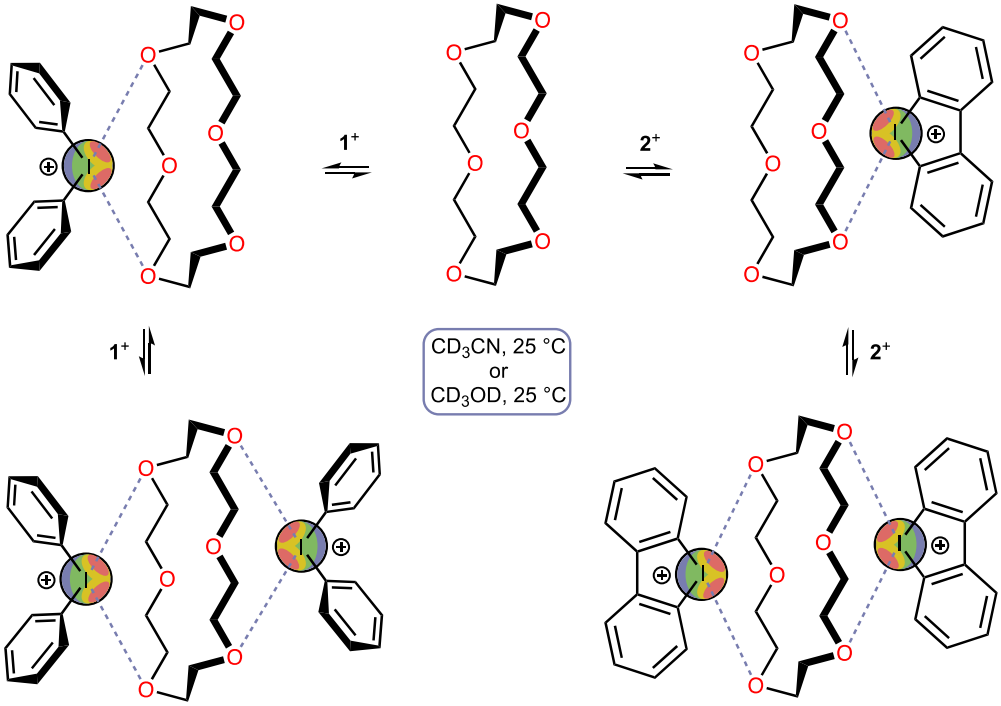

Scheme 2. Simplified representation of a plausible association of the iodine(III)-containing Lewis acids with 18-crown-6 and the conditions utilized for the ^{1}H NMR titration. The counter-ions are omitted for clarity.

Although both cyclic and acyclic iodononium salts previously exhibited excellent titration curves during the study of their binding with a series of simple nucleophiles in protic and aprotic solvents,[4, 5, 7, 8] the titration of 18-crown-6 with **1**^{OTf} or **2**^{OTf} exhibited

some peculiarities. Thus, in CD_3CN, the titration of 18-crown-6 with cyclic $\mathbf{2}^{OTf}$ showed points excellently fitted by the approximation curve (**Figure 1**, top, red line) related to K^{298} = 8.3(4) M^{-1} (1:1 associate), whereas the data obtained for acyclic $\mathbf{1}^{OTf}$ was impossible to fit in the 1:1 or 1:2 approximation models due to counter-directional changes in the chemical shift of 18-crown-6 signal at low and high ratios of the iodonium salt (**Figure 1**, top, blue line). Similar counter-directionality in chemical shift displacement was previously observed by Beer, Langton and co-workers[26] during the titration of multidentate iodine(I)-derived halogen bond donors with chloride, and the authors suggested that this observation is due to a change in the reagent association ratio. Considering this, the obtained in CD_3CN data might indicate the exclusive formation of 1:1 associates of 18-crown-6 with $\mathbf{2}^{OTf}$, and the formation of 1:1 associates 18C6·$\mathbf{1}^{OTf}$ at low concentrations of $\mathbf{1}^{OTf}$ and 1:2 associates at higher values of 18C6:$\mathbf{1}^{OTf}$ ratio. Crystals of the $\mathbf{1}^{OTf}$·18C6·$\mathbf{1}^{OTf}$ associate suitable for XRD study were also prepared via slow evaporation of the mixture of 18-crown-6 and $\mathbf{1}^{OTf}$ (1:2 molar ratio) dissolved in MeCN at room temperature in air (**Figure 2**).

In CD_3OD, titration of 18-crown-6 with $\mathbf{1}^{OTf}$ led to the data being well fitted by the 1:1 host–guest binding model giving K^{298} = 18(3) M^{-1}, whereas the titration with $\mathbf{2}^{OTf}$ was impossible to fit with sufficient accuracy in any association model, which might indicate a low value of the corresponding binding constant. The gradual change in chemical shift in this case should be attributed to the change of media during the increase in the ratio of $\mathbf{2}^{OTf}$.

Taking into account all these experimental observations, it can be concluded that acyclic cation $\mathbf{1}^{OTf}$ exhibits higher affinity to 18-crown-6 in both chosen solvents compared to $\mathbf{2}^{OTf}$, and the binding is more energetically profitable in CD_3CN compared with CD_3OD.

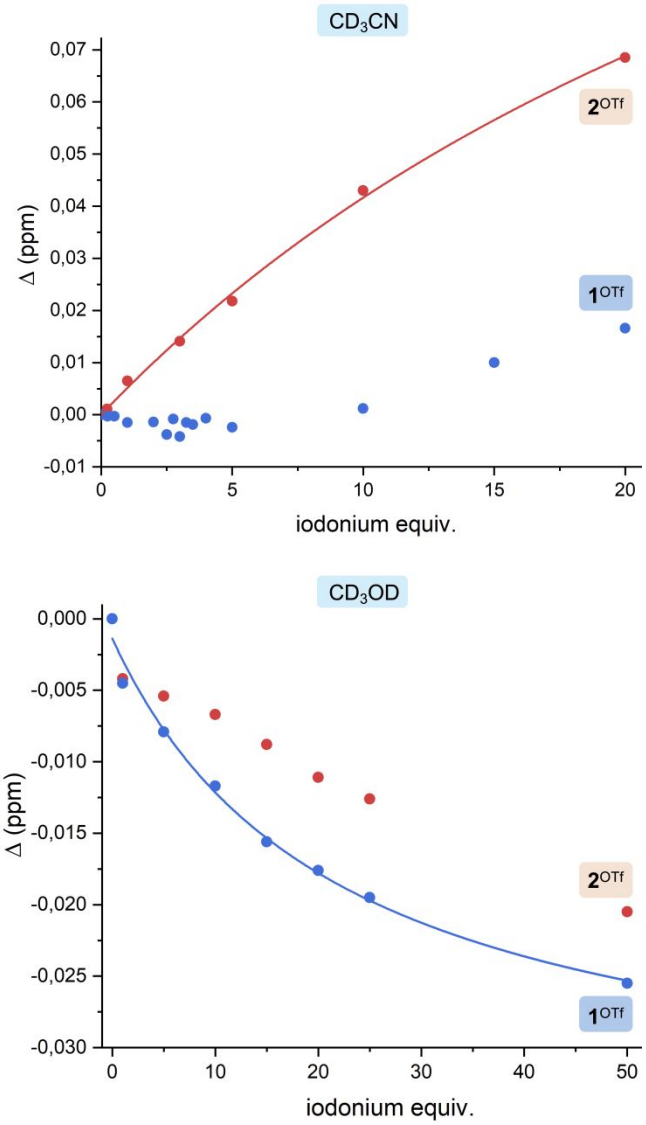

Figure 1. Experimental ^{1}H NMR titration points and calculated curves of mixtures of **1**^{OTf} or **2**^{OTf} with 18-crown-6. The plot represents the shift of the resonance peak of the 18-crown-6. The approximation curves and the corresponding K^{298} values were calculated using Bindfit software using a 1:1 host–guest binding model.

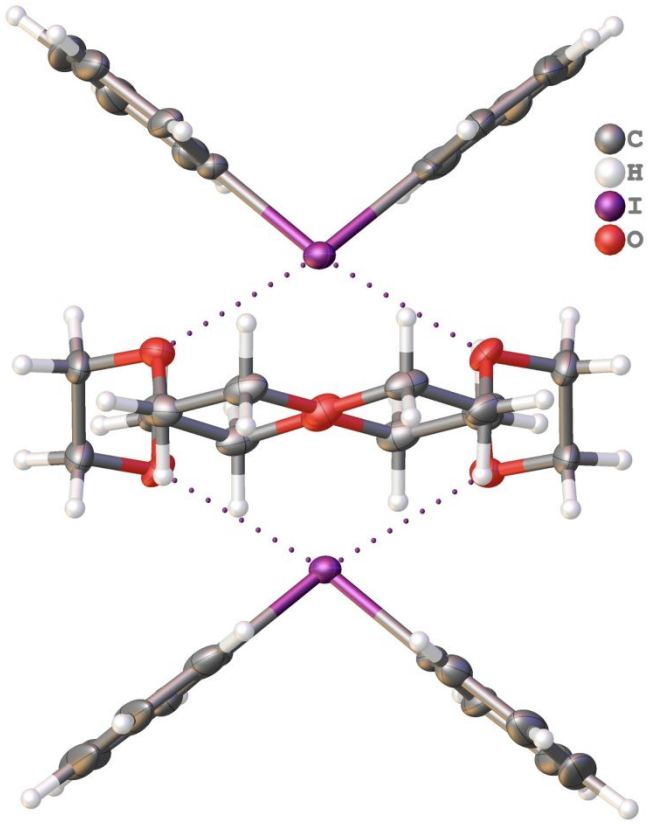

Figure 2. A thermal ellipsoid plot for $\mathbf{1}^{OTf}$·18C6·$\mathbf{1}^{OTf}$. Two triflate anions are omitted for clarity. Thermal ellipsoids are given at the 50% probability level.

Theoretical study. To better understand the reason for the inversion of relative binding constants for acyclic and cyclic iodonium salts relatively to previously published results, the corresponding DFT calculations have been carried out (see Computational Details). In the computational model, the triflate anion was omitted, as most of the effects from the counter-anion are absorbed by solvation correction.[27] The obtained results turned out to be in qualitative agreement with the experimentally obtained data (**Table 1**). In all cases, binding of 18-crown-6 with acyclic $\mathbf{1}^+$ is more energetically favorable than the binding with cyclic $\mathbf{2}^+$. Moreover, in MeCN, formation of 1:1 associate $\mathbf{2}^+$·18C6 has comparable value of the Gibbs free energy with the formation of 1:2 associate $\mathbf{1}^+$·18C6·$\mathbf{1}^+$, which confirms the suggestion made based on the experimental data. In both solvents, the formation of $\mathbf{2}^+$·18C6·$\mathbf{2}^+$ is clearly unfavorable under the studied conditions, which explains good fitting of the experimental plot for 1:1 association in the case of a high concentration of $\mathbf{2}^+$ in MeCN.

Table 1. Calculated values of Gibbs free energies of reaction for model processes $\Delta G = G_{product} - \Sigma G_{reactants}$. Calculated total electronic energies, enthalpies, Gibbs free energies,

and entropies for all optimized equilibrium model structures are given in Supporting Information.

Model association	ΔG, kJ mol^{-1}	
	MeCN	MeOH
1$^+$ + 18C6 → **1**$^+$·18C6	–15.9	–14.3
2$^+$ + 18C6 → **2**$^+$·18C6	–4.9	–10.7
1$^+$ + **1**$^+$ + 18C6 → **1**$^+$·18C6·**1**$^+$	–2.8	–6.0
2$^+$ + **2**$^+$ + 18C6 → **2**$^+$·18C6·**2**$^+$	25.0	7.7

To visualize intermolecular interactions in the optimized equilibrium model structures **1**$^+$·18C6, **2**$^+$·18C6, **1**$^+$·18C6·**1**$^+$, and **2**$^+$·18C6·**2**$^+$, the noncovalent interactions analysis (NCI)[28] was additionally performed for model supramolecular associates (**Figure 2**). The iodonium cations interact with the whole molecule of the crown ether, and it is difficult to definitely identify any dominant type of noncovalent interactions in such chemical systems via this method, particularly in the solution state. In fact, all the contacts I···O could be classified as weak interactions, but a minority of them can be classified as halogen bonds due to their failure to meet geometric criteria. Nevertheless, the NCI analysis indicated that acyclic iodonium cation forms higher number of noncovalent interactions with the crown ether (**Figure 2**, top) than its cyclic analogue (**Figure 2**, bottom), due to the interactions of 18-crown-6 with the π-system of the phenyl rings. Such types of interactions have been theoretically observed by us previously for other onium salts.[29]

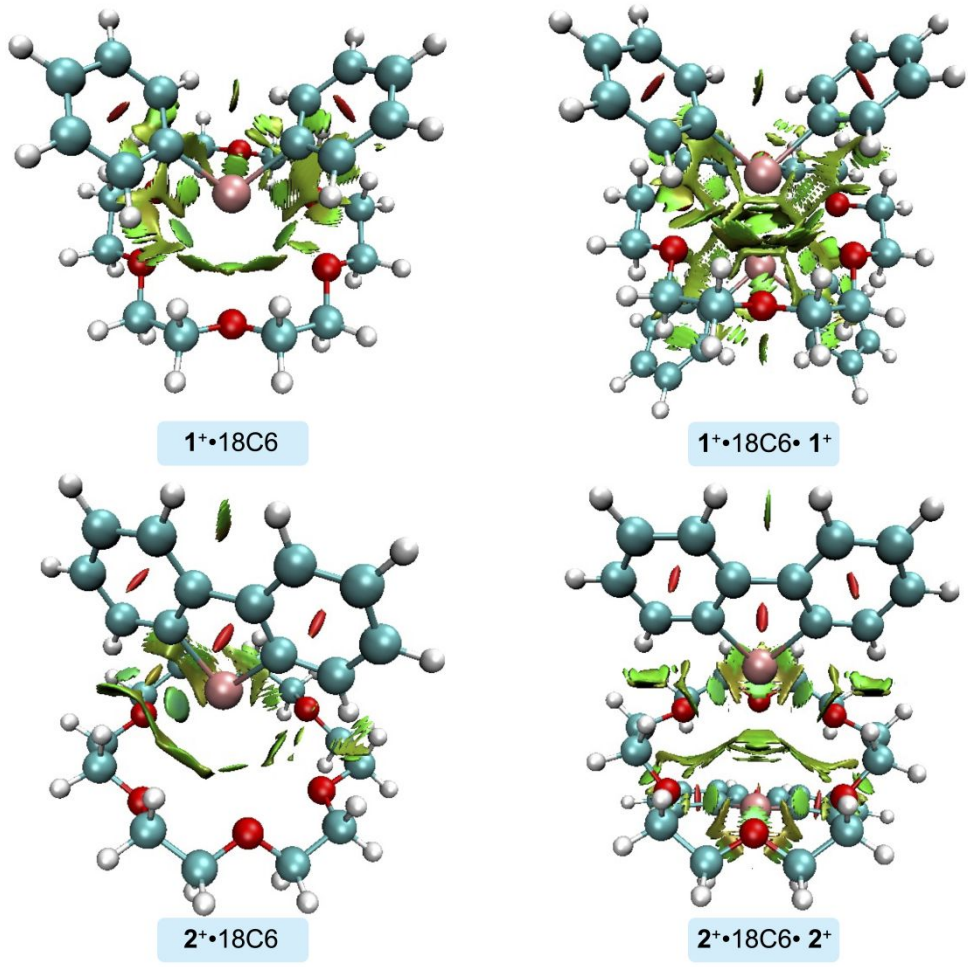

Figure 2. Visualization of intermolecular contacts in calculated structures of the associates **1**$^{+}$·18C6, **2**$^{+}$·18C6, **1**$^{+}$·18C6·**1**$^{+}$, and **2**$^{+}$·18C6·**2**$^{+}$ using NCI analysis technique.

To estimate the relative energy of weak interactions, QTAIM analysis has been performed for model associates **1**$^{+}$·18C6 and **2**$^{+}$·18C6 (**Table 2**). The obtained data indicate that the total estimated energy of all weak interactions between two species in **1**$^{+}$···18C6 equals to 64.3 kJ mol^{-1} those value consists of 24.9 kJ mol^{-1} contribution of two normal halogen bonds, 23.6 kJ mol^{-1} contribution of other four I···O contacts, and additionally 15.7 kJ mol^{-1} from the phenyl···crown interactions. For **2**$^{+}$···18C6, total energy of binding is 52.6 kJ mol^{-1}, which consists of 31.6 kJ mol^{-1} contribution of one hybrid halogen and hydrogen bond and 21.0 kJ mol^{-1} for other five I···O contacts. These data are in full agreement with the experimentally obtained data indicating that **1**$^{+}$ binds the crown ether more efficiently than **2**$^{+}$.

Table 2. Values of the density of all electrons – $\rho(\mathbf{r})$, Laplacian of electron density – $\nabla^2\rho(\mathbf{r})$ and appropriate λ_2 eigenvalues, energy density – H_b, potential energy density – $V(\mathbf{r})$, Lagrangian kinetic energy – $G(\mathbf{r})$, and electron localization function – ELF (a.u.) at the

bond critical points (3, –1), corresponding to selected noncovalent interactions in model supramolecular associates **1**$^{+}$•18C6 and **2**$^{+}$•18C6 (methanol solution), and estimated strength for these weak contacts E_{int} (kJ/mol).

Contact	Bond distance (Å)	$\rho(\mathbf{r})$	$\nabla^2\rho(\mathbf{r})$	λ_2	H_b	$V(\mathbf{r})$	$G(\mathbf{r})$	ELF	$E_{int} \approx -V(\mathbf{r})/2$
1^{+}•18C6									
I···O	3.047	0.015	0.055	–0.015	0.000	–0.011	0.011	0.045	14.4
	3.183	0.011	0.042	–0.011	0.001	–0.008	0.009	0.032	10.5
	3.308	0.010	0.037	–0.010	0.001	–0.007	0.008	0.031	9.2
	3.545	0.007	0.024	–0.007	0.001	–0.004	0.005	0.017	5.3
	3.607	0.006	0.022	–0.006	0.001	–0.004	0.005	0.018	5.3
	3.644	0.005	0.019	–0.005	0.001	–0.003	0.004	0.011	3.9
C_{Ph}···H	2.744	0.007	0.024	–0.007	0.001	–0.004	0.005	0.027	5.3
	2.743	0.007	0.025	–0.007	0.002	–0.003	0.005	0.023	3.9
	2.838	0.007	0.022	–0.007	0.001	–0.003	0.004	0.022	3.9
	2.849	0.006	0.019	–0.006	0.002	–0.002	0.004	0.019	2.6
2^{+}•18C6									
I···O	2.963	0.017	0.066	–0.017	0.001	–0.012	0.013	0.055	15.8
	3.474	0.007	0.028	–0.007	0.001	–0.005	0.006	0.020	6.6
	3.523	0.007	0.026	–0.007	0.001	–0.004	0.005	0.018	5.3
	3.643	0.005	0.019	–0.005	0.001	–0.003	0.004	0.013	3.9
	3.619	0.005	0.020	–0.005	0.001	–0.003	0.004	0.013	3.9
	3.867	0.003	0.012	–0.003	0.001	–0.001	0.002	0.004	1.3
H···O	2.295	0.015	0.049	–0.015	0.000	–0.012	0.012	0.046	15.8

Conclusion

In this work, we have shown that relative ability to bind nucleophilic species of cyclic and acyclic iodonium salts depends on the nature of model nucleophile chosen for the study. The major part of articles dealing with the titration of halogen bond donors typically utilize simple unbulky nucleophilic agents like halides or *C*-, *N*-, or *O*-donors.[4, 21] In these cases, cyclic iodonium salts exhibit higher values of binding constants due to ability to form bifurcate halogen and hydrogen bonding with the Lewis base which is stronger than conventional halogen bonding in the case of acyclic iodonium salts (**Table 2**). Nevertheless, in the case of association with a bulky Lewis base, structural flexibility of acyclic iodonium cations allows them to better associate with the base since the σ-holes of the cation are more accessible for the interaction, whereas the phenyl π-system might provide additional binding of the nucleophilic agent (**Scheme 3**).

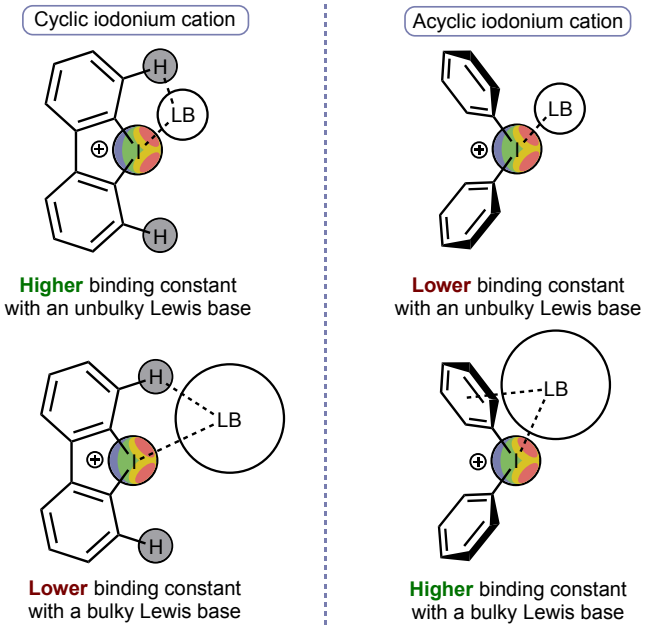

Scheme 3. Binding of cyclic and acyclic iodonium salts with unbulky and bulky Lewis base.

Taking these observations into account, it should be concluded that the utilization of acyclic iodonium salts instead of their cyclic analogues might be a rational choice for the catalysis of organic transformations involving bulky substrates and/or proceeding via bulky transition states.

Experimental Section

Materials and instrumentation. All solvents and reagents were obtained from commercial sources and used as received. The diphenyliodonium and dibenziodolium triflates were synthesized according to published procedure.[4] All syntheses were conducted in air. ^{1}H NMR spectra were measured on a Bruker Avance 400 spectrometer in CD_3CN and CD_3OD at 298 K; the residual solvent signal was used as the internal standard. The electrospray ionization mass-spectra were obtained on a Bruker maXis spectrometer equipped with an electrospray ionization (ESI) source. The instrument was operated in a positive ion mode using an *m*/*z* range 100–1000. The nebulizer gas flow was 1.0 bar and the drying gas flow 4.0 L min^{-1}. For HRESI$^+$, the studied compounds were dissolved in MeOH.

^{1}H NMR titration data. To a series of mixtures of 18-Crown-6 (0.037 M, 50 μL) and diphenyliodonium triflate or dibenziodolium triflate (up to 50-fold excess; see Supporting Information) in NMR tubes, CD_3CN or CD_3OD wasadded to achieve a volume of resulting

solution equal to 500 μL. The 18-Crown-6 signal was used to track the changes in the chemical shift in ^{1}H NMR spectra during variation of the iodonium salt concentration.

Syntheses of the iodonium salts. *Diphenyliodonium triflate (**1**^{OTf}). m*-CPBA (77 %, 1.5 equiv, 6 mmol, 1.348 g) and TfOH (3.0 equiv, 12 mmol, 1.061 mL) were added to a stirred solution of iodobenzene (1.0 equiv, 4 mmol, 0.448 mL) and benzene (1.0 equiv, 4 mmol, 0.355 mL) in dry CH_2Cl_2 (10 mL) and the resulting solution was stirred for 1 h at RT. Then the solvent was evaporated *in vacuo* at RT, and the product was crystallized using Et_2O (10 mL). The obtained heterogeneous solution was stirred for 20 min at RT and then the solid phase was filtered off, washed with Et_2O (10 mL), and dried at 50 °C in air.

White crystalline solid. Yield: 82 % (1.41 g). M.p.: 168–170 °C. δ = 8.28 – 8.26 (m, 4H), 7.67 – 7.63 (m, 2H), 7.55 – 7.51 (m, 4H). ^{13}C{^{1}H} NMR (100.61 MHz, $(CD_3)_2SO$): δ = 135.66, 132.50, 132.21, 116.93 (Ar), 121.23 (q, $^1J_{CF}$ = 322.3 Hz, *C*F$_3$). ^{19}F NMR (376.49 MHz, CD_3CN): δ = –79.26 (s, C*F*$_3$). HRMS (ESI-TOF): *m/z* [M]$^+$ calcd for $C_{12}H_{10}I$: 280.9822; found: 280.9819.

*Dibenziodolium triflate (**2**^{OTf}). m*-CPBA (77 %, 1.5 equiv, 2.96 mmol, 665 mg) and TfOH (3.0 equiv, 5.89 mmol, 0.521 mL) were added to a stirred solution of 2-iodo-1,1'-biphenyl (1.0 equiv, 1.97 mmol, 550 mg) in dry CH_2Cl_2 (5 mL) and stirred for 1 h at RT. Then the solvent was evaporated *in vacuo* at RT, and the product was crystallized using Et_2O (10 mL). The obtained heterogeneous solution was stirred for 20 min at RT and then the solid phase was filtered off, washed with Et_2O (10 mL), and dried at 50 °C in air.

White crystalline solid. Yield: 90 % (760 mg). M.p.: 240–242 °C. ^{1}H NMR (400.13 MHz, $(CD_3)_2SO$): δ = 8.37 (dd, $^3J_{HH}$ = 8.1 Hz, $^4J_{HH}$ = 1.5 Hz, 2H, Ar), 8.15 (d, $^3J_{HH}$ = 8.1 Hz, 2H, Ar), 7.79 (t, $^3J_{HH}$ = 7.8 Hz, 2H, Ar), 7.67 (td, $^3J_{HH}$ = 7.8 Hz, $^4J_{HH}$ = 1.5 Hz, 2H, Ar). ^{13}C{^{1}H} NMR (100.61 MHz, $(CD_3)_2SO$): δ = 142.1, 131.5, 131.1, 131.0, 127.4, 121.9 (Ar), 121.2 (q, $^1J_{CF}$ = 322.3 Hz, *C*F$_3$). ^{19}F NMR (376.49 MHz, CD_3CN): δ = −79.25 (s, C*F*$_3$). HRMS (ESI-TOF): *m/z* [M]$^+$ calcd for $C_{12}H_8I$: 278.9665; found: 278.9670.

Computational details. The full geometry optimization procedure with UFF pre-optimization in Avogadro program package (https://avogadro.cc/) for all model structures was carried out at the DFT level of theory using the hybrid functional ωB97XD[30] (the addition of dispersion correction is *de facto* a standard practice in modern computational chemistry, and it was automatically internally employed in the functional ωB97XD specifically developed for these purposes) with the help of Gaussian-09[31] program package (revision C.01). The iodine is a heavy and relativistic atom and application of special basis sets and pseudopotentials for proper description of the properties of such atoms are highly desirable. By this reason, we used the quasi-relativistic MWB46

pseudopotentials, which described 46 core electrons, and the appropriate contracted basis sets for iodine atoms,[32] while the standard 6-311G* basis sets were used for all other atoms. Note that it is well known from many original articles and benchmark studies[33-36] that triple-zeta quality basis sets (including 6-311G*) are good enough and produce very small basis set superposition errors. No symmetry restrictions were applied during the geometry optimization procedure. The solvent effects were taken into account using the SMD (Solvation Model based on Density) continuum solvation model suggested by Truhlar and coworkers[37] for methanol and acetonitrile as solvents. We used standard default settings for SMD model implemented in Gaussian-09 program package (revision C.01) – atomic radii: SMD-Coulomb, atomic radii for non-electrostatic terms: SMD-CDS, cavity type: VdW (van der Waals surface), cavity algorithm: GePol, solvents: acetonitrile (Eps = 35.688; Eps(inf) = 1.806874) and methanol (Eps = 32.613; Eps(inf) = 1.765709). The Hessian matrices were calculated analytically for all optimized model structures to prove the location of the correct minimum on the potential energy surface (no imaginary frequencies were found in all cases) and to estimate the thermodynamic parameters, the latter being calculated at 298 K and 1 atm. The noncovalent interactions analysis (NCI) have been performed by using the Multiwfn program (version 3.7),[38] and visualized by using the VMD program.[39] The topological analysis of the electron density distribution in model structures within the “atoms in molecules” (QTAIM) method[40] was performed by using the Multiwfn program[38] (version 3.7). The Cartesian atomic coordinates for all model structures are presented in the attached xyz-file, Supporting Information.

Single-crystal XRD study. Single-crystal X-ray diffraction experiment was carried out on Agilent Technologies «SuperNova» diffractometer with monochromated CuKα radiation. Crystals were kept at 100(2) K during data collection. Structure have been solved by the Superflip[41, 42] and the ShelXT[43] structure solution programs using Charge Flipping and Intrinsic Phasing and refined by means of the ShelXL[44] program incorporated in the OLEX2[45] program package. The crystal data and details of structure refinements for **1**^{OTf}·18C6·**1**^{OTf} are shown in **Table S6**. The structures can be obtained free of charge via the Cambridge Crystallographic Database (CCDC 2361448; https://www.ccdc.cam.ac.uk/structures/).

Conflict of interest

There are no conflicts to declare.

Supporting Information

Titration data; Spectra of the iodonium salts; Calculation data; Crystal data for $\mathbf{1}^{OTf}\cdot18C6\cdot\mathbf{1}^{OTf}$ (**PDF**)

Optimized model structures (**XYZ**)

Acknowledgements

This work was supported by the Saint Petersburg State University (grant 103922061 — synthetic work) and RUDN University Scientific Projects Grant System (project No 021342-2-000 — DFT calculations). Physicochemical studies were performed at the Center for Magnetic Resonance, and Center for Chemical Analysis and Materials Research (all at Saint Petersburg State University).

Author ORCIDs:

Alexandra A. Sysoeva: 0000-0003-2317-6095

Alexander S. Novikov: 0000-0001-9913-5324

Mikhail V. Il'in: 0000-0003-4234-4779

Dmitrii S. Bolotin: 0000-0002-9612-3050

References

1. X. Peng, A. Rahim, W. Peng, F. Jiang, Z. Gu and S. Wen, *Chem. Rev.*, 2023, **123**, 1364–1416.
2. Y. Zhang, J. Han and Z.-J. Liu, *RSC Adv.*, 2015, **5**, 25485–25488.
3. F. Heinen, D. L. Reinhard, E. Engelage and S. M. Huber, *Angew. Chem. Int. Ed.*, 2021, **60**, 5069–5073.
4. M. V. Il'in, A. A. Sysoeva, A. S. Novikov and D. S. Bolotin, *J. Org. Chem.*, 2022, **87**, 4569–4579.
5. M. V. Il'in, D. A. Polonnikov, A. S. Novikov, A. A. Sysoeva, Y. V. Safinskaya and D. S. Bolotin, *ChemPlusChem*, 2023, **88**, e202300304.
6. D. A. Polonnikov, M. V. Il'in, Y. V. Safinskaya, I. S. Aliyarova, A. S. Novikov and D. S. Bolotin, *Org. Chem. Front.*, 2023, **10**, 169–180.
7. A. A. Sysoeva, M. V. Il'in and D. S. Bolotin, *ChemCatChem*, 2024, DOI: 10.1002/cctc.202301668, e202301668.

8. S. N. Yunusova, A. S. Novikov, N. S. Soldatova, M. A. Vovk and D. S. Bolotin, *RSC Adv.*, 2021, **11**, 4574–4583.
9. A. A. Sysoeva, A. S. Novikov, M. V. Il'in and D. S. Bolotin, *Catal. Sci. Technol.*, 2023, **13**, 3375–3385.
10. D. L. Reinhard, F. Heinen, J. Stoesser, E. Engelage and S. M. Huber, *Helv. Chim. Acta*, 2021, **104**, e2000221.
11. F. Heinen, E. Engelage, A. Dreger, R. Weiss and S. M. Huber, *Angew. Chem. Int. Ed.*, 2018, **57**, 3830–3833.
12. Y. Nishida, T. Suzuki, Y. Takagi, E. Amma, R. Tajima, S. Kuwano and T. Arai, *ChemPlusChem*, 2021, **86**, 741–744.
13. R. Haraguchi, T. Nishikawa, A. Kanazawa and S. Aoshima, *Macromolecules*, 2020, **53**, 4185–4192.
14. Y. Yoshida, T. Fujimura, T. Mino and M. Sakamoto, *Adv. Synth. Catal.*, 2022, **364**, 1091–1098.
15. J. Wolf, F. Huber, N. Erochok, F. Heinen, V. Guerin, C. Y. Legault, S. F. Kirsch and S. M. Huber, *Angew. Chem. Int. Ed.*, 2020, **59**, 16496–16500.
16. M. V. Il'in, Y. V. Safinskaya, D. A. Polonnikov, A. S. Novikov and D. S. Bolotin, *J. Org. Chem.*, 2024, **89**, 2916–2925.
17. X. Han, H. B. Zhou and C. Dong, *Chem. Rec.*, 2016, **16**, 897–906.
18. T. James, M. van Gemmeren and B. List, *Chem. Rev.*, 2015, **115**, 9388–9409.
19. Y. Qin, L. Zhu and S. Luo, *Chem. Rev.*, 2017, **117**, 9433–9520.
20. B. Han, X. H. He, Y. Q. Liu, G. He, C. Peng and J. L. Li, *Chem. Soc. Rev.*, 2021, **50**, 1522–1586.
21. R. J. Mayer, A. R. Ofial, H. Mayr and C. Y. Legault, *J. Am. Chem. Soc.*, 2020, **142**, 5221–5233.
22. M. Ochiai, K. Miyamoto, T. Suefuji, S. Sakamoto, K. Yamaguchi and M. Shiro, *Angew. Chem. Int. Ed.*, 2003, **42**, 2191–2194.
23. M. Ochiai, K. Miyamoto, M. Shiro, T. Ozawa and K. Yamaguchi, *J. Am. Chem. Soc.*, 2003, **125**, 13006–13007.
24. M. Ochiai, K. Miyamoto, T. Suefuji, M. Shiro, S. Sakamoto and K. Yamaguchi, *Tetrahedron*, 2003, **59**, 10153–10158.
25. M. Ochiai, T. Suefuji, K. Miyamoto, N. Tada, S. Goto, M. Shiro, S. Sakamoto and K. Yamaguchi, *J. Am. Chem. Soc.*, 2003, **125**, 769–773.
26. A. Docker, X. Shang, D. Yuan, H. Kuhn, Z. Zhang, J. J. Davis, P. D. Beer and M. J. Langton, *Angew. Chem. Int. Ed.*, 2021, **60**, 19442–19450.

27. P. Erdmann, M. Schmitt, L. M. Sigmund, F. Kramer, F. Breher and L. Greb, *Angew. Chem. Int. Ed.*, 2024, DOI: 10.1002/anie.202403356, e202403356.
28. E. R. Johnson, S. Keinan, P. Mori-Sanchez, J. Contreras-Garcia, A. J. Cohen and W. Yang, *J. Am. Chem. Soc.*, 2010, **132**, 6498–6506.
29. A. S. Novikov and D. S. Bolotin, *Org. Biomol. Chem.*, 2022, **20**, 7632–7639.
30. J. D. Chai and M. Head-Gordon, *Phys. Chem. Chem. Phys.*, 2008, **10**, 6615–6620.
31. M. J. Frisch, G. W. Trucks, H. B. Schlegel, G. E. Scuseria, M. A. Robb, J. R. Cheeseman, G. Scalmani, V. Barone, B. Mennucci, G. A. Petersson, H. Nakatsuji, M. Caricato, X. Li, H. P. Hratchian, A. F. Izmaylov, J. Bloino, G. Zheng, J. L. Sonnenberg, M. Hada, M. Ehara, K. Toyota, R. Fukuda, J. Hasegawa, M. Ishida, T. Nakajima, Y. Honda, O. Kitao, H. Nakai, T. Vreven, J. J. A. Montgomery, J. E. Peralta, F. Ogliaro, M. Bearpark, J. J. Heyd, E. Brothers, K. N. Kudin, V. N. Staroverov, T. Keith, R. Kobayashi, J. Normand, K. Raghavachari, A. Rendell, J. C. Burant, S. S. Iyengar, J. Tomasi, M. Cossi, N. Rega, J. M. Millam, M. Klene, J. E. Knox, J. B. Cross, V. Bakken, C. Adamo, J. Jaramillo, R. Gomperts, R. E. Stratmann, O. Yazyev, A. J. Austin, R. Cammi, C. Pomelli, J. W. Ochterski, R. L. Martin, K. Morokuma, V. G. Zakrzewski, G. A. Voth, P. Salvador, J. J. Dannenberg, S. Dapprich, A. D. Daniels, O. Farkas, J. B. Foresman, J. V. Ortiz, J. Cioslowski and D. J. Fox, *Gaussian 09, Revision C.01*, 2010.
32. A. Bergner, M. Dolg, W. Küchle, H. Stoll and H. Preuß, *Mol. Phys.*, 1993, **80**, 1431–1441.
33. B. Paizs and S. Suhai, *J. Comput. Chem.*, 1998, **19**, 575–584.
34. A. Vidal Vidal, L. C. de Vicente Poutas, O. Nieto Faza and C. S. Lopez, *Molecules*, 2019, **24**, 3810.
35. M. Gray, P. E. Bowling and J. M. Herbert, *J. Chem .Theory Comput.*, 2022, **18**, 6742–6756.
36. R. Crespo-Otero, L. A. Montero, W. D. Stohrer and J. M. Garcia de la Vega, *J. Chem. Phys.*, 2005, **123**, 134107.
37. A. V. Marenich, C. J. Cramer and D. G. Truhlar, *J. Phys. Chem. B*, 2009, **113**, 6378–6396.
38. T. Lu and F. Chen, *J. Comput. Chem.*, 2012, **33**, 580–592.
39. W. Humphrey, A. Dalke and K. Schulten, *J. Mol. Graph.*, 1996, **14**, 33–38.
40. R. F. W. Bader, *Chem. Rev.*, 1991, **91**, 893–928.
41. L. Palatinus and G. Chapuis, *J. Appl. Crystallogr.*, 2007, **40**, 786–790.

42. L. Palatinus, S. J. Prathapa and S. van Smaalen, *J. Appl. Crystallogr.*, 2012, **45**, 575–580.
43. G. M. Sheldrick, *Acta Crystallogr.*, 2015, **A71**, 3–8.
44. G. M. Sheldrick, *Acta Crystallogr.*, 2015, **C71**, 3–8.
45. O. V. Dolomanov, L. J. Bourhis, R. J. Gildea, J. A. K. Howard and H. Puschmann, *J. Appl. Crystallogr.*, 2009, **42**, 339–341.

TOC entry

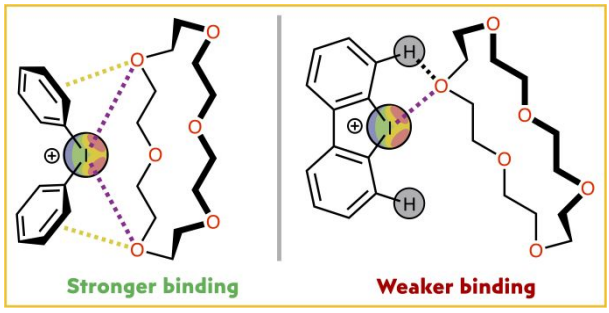

Acyclic diphenyliodonium cation forms stronger interactions with the bulky Lewis base than cyclic dibenziodolium cation.

SUPPORTING INFORMATION

Halogen Bonded Associates of Iodonium Salts with 18-Crown-6: Does Structural Flexibility or Structural Rigidity of the σ-Hole Donor Provide Efficient Substrate Ligation?

Alexandra A. Sysoeva,[1] Alexander S. Novikov,[1,2] Mikhail V. Il'in,[1] and Dmitrii S. Bolotin[1,*]

[1] Institute of Chemistry, Saint Petersburg State University, Universitetskaya Nab. 7/9, Saint Petersburg, 199034, Russian Federation

[2] Peoples' Friendship University of Russia (RUDN University), Miklukho-Maklaya Str. 6, 117198 Moscow, Russian Federation

* Corresponding author E-mail: d.s.bolotin@spbu.ru

Table of contents

Titration data

Table S1. Titration data of dibenziodolium triflate in CD_3CN.

Equivalents of dibenziodolium triflate	δ, ppm	Δδ, ppm
0	3.539	0.000
0.25	3.540	0.001
1	3.546	0.006
3	3.553	0.014
5	3.561	0.022
10	3.582	0.043
20	3.608	0.069

Table S2. Titration data of diphenyliodonium triflate in CD_3CN.

Equivalents of diphenyliodonium triflate	δ, ppm	Δδ, ppm
0	3.539	0.000
0.25	3.539	0.000
0.5	3.539	0.000
1	3.538	-0.002
2	3.538	-0.001
2.5	3.536	-0.004
2.75	3.539	-0.001
3	3.535	-0.004
3.25	3.538	-0.002
3.5	3.537	-0.002
4	3.539	-0.001
5	3.537	-0.002
10	3.541	0.001
15	3.549	0.010
20	3.556	0.017

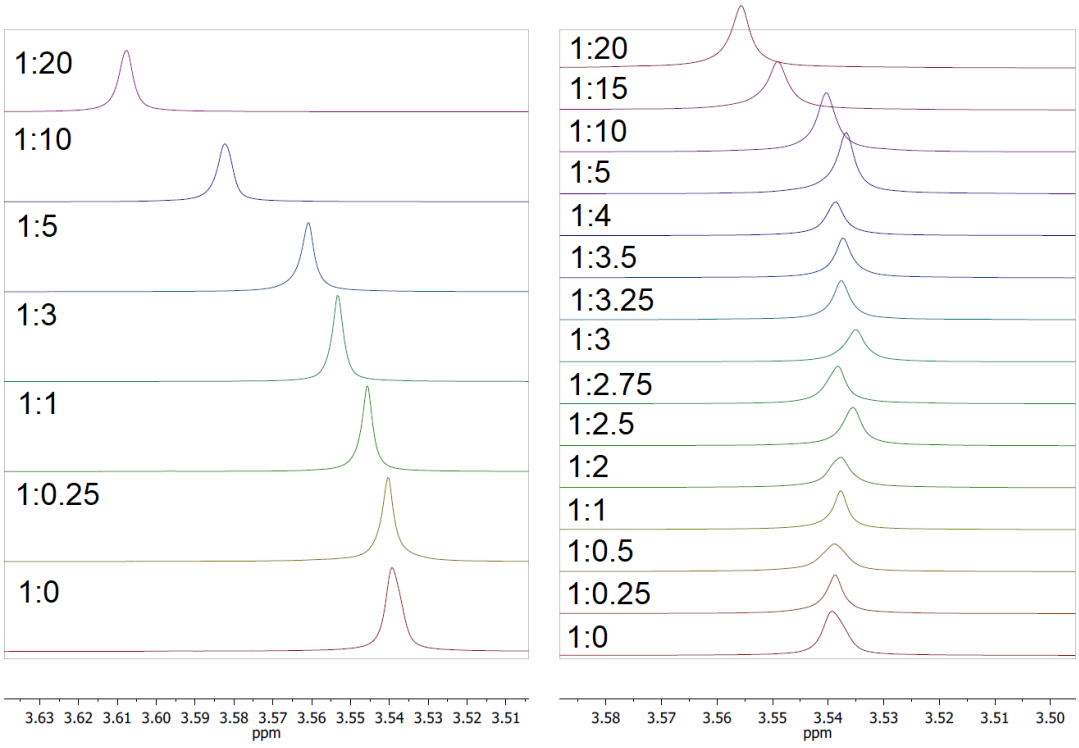

Figure S1. Stacked ^1H NMR spectra for the titration of 18-crown-6 with dibenziodolium triflate (left) or diphenyliodonium triflate (right) in CD_3CN.

Table S3. Titration data of dibenziodolium triflate in CD_3OD.

Equivalents of dibenziodolium triflate	δ, ppm	Δδ, ppm
0	3.660	0.000
1	3.656	-0.004
5	3.655	-0.005
10	3.653	-0.007
15	3.651	-0.009
20	3.649	-0.011
25	3.647	-0.013
50	3.639	-0.020

Table S4. Titration data of diphenyliodonium triflate in CD_3OD.

Equivalents of diphenyliodonium triflate	δ, ppm	Δδ, ppm
0	3.660	0.000
1	3.655	-0.004
5	3.652	-0.008
10	3.648	-0.012
15	3.644	-0.016
20	3.642	-0.018
25	3.640	-0.019
50	3.634	-0.026

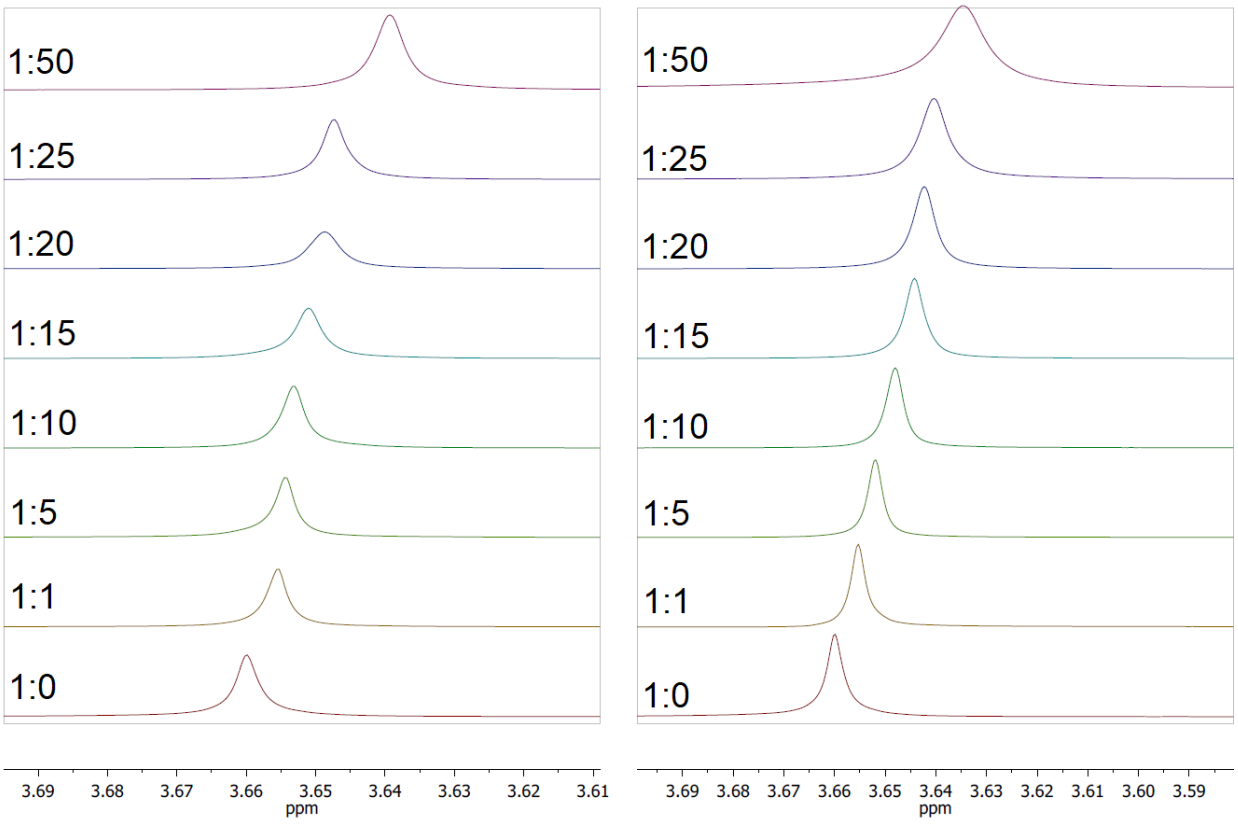

Figure S2. Stacked ^1H NMR spectra titration of dibenziodolium triflate (left) and diphenyliodonium triflate (right) in CD_3OD.

Spectra of the iodonium salts

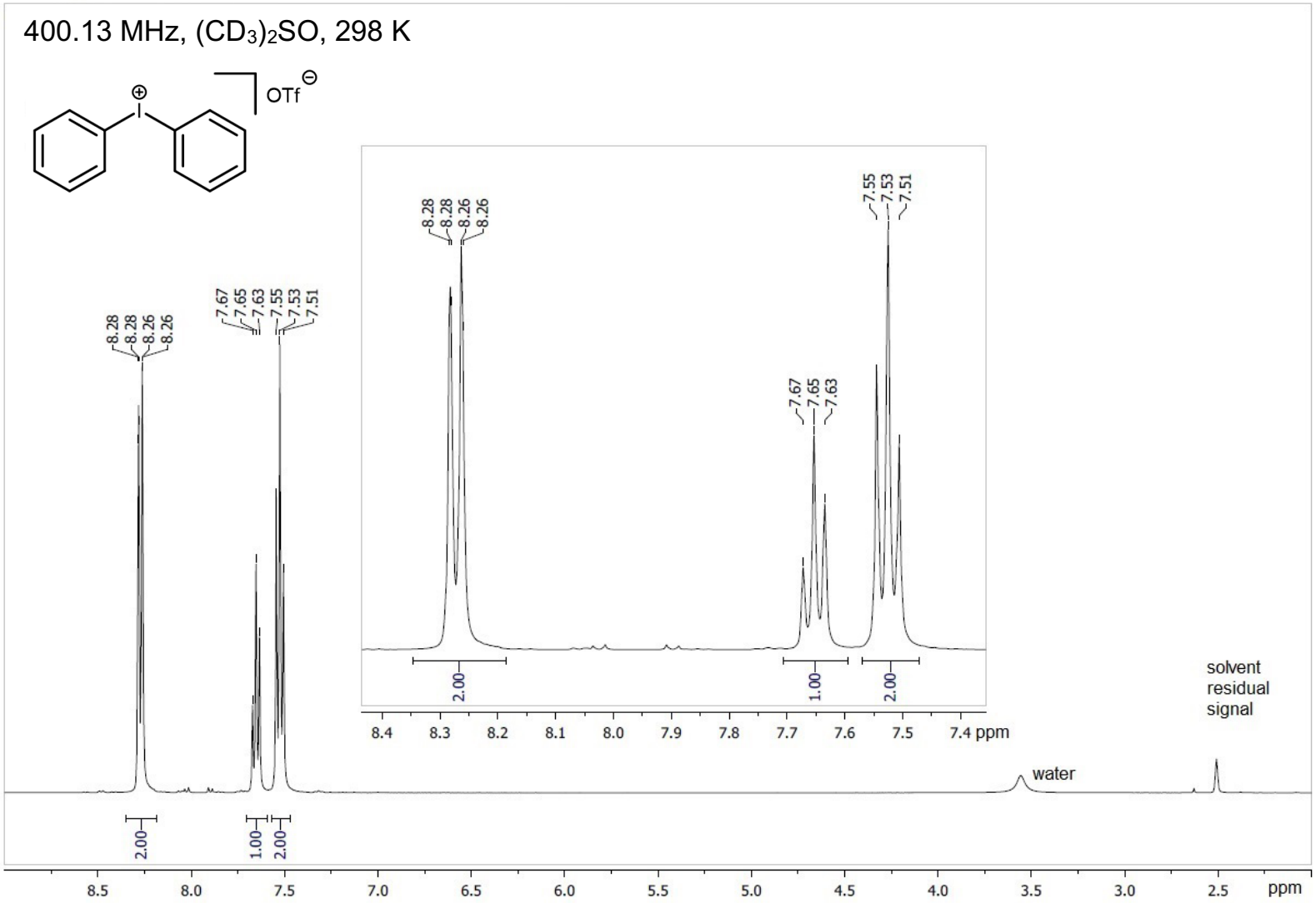

Figure S3. ^{1}H NMR spectrum of the **1**^{OTf}.

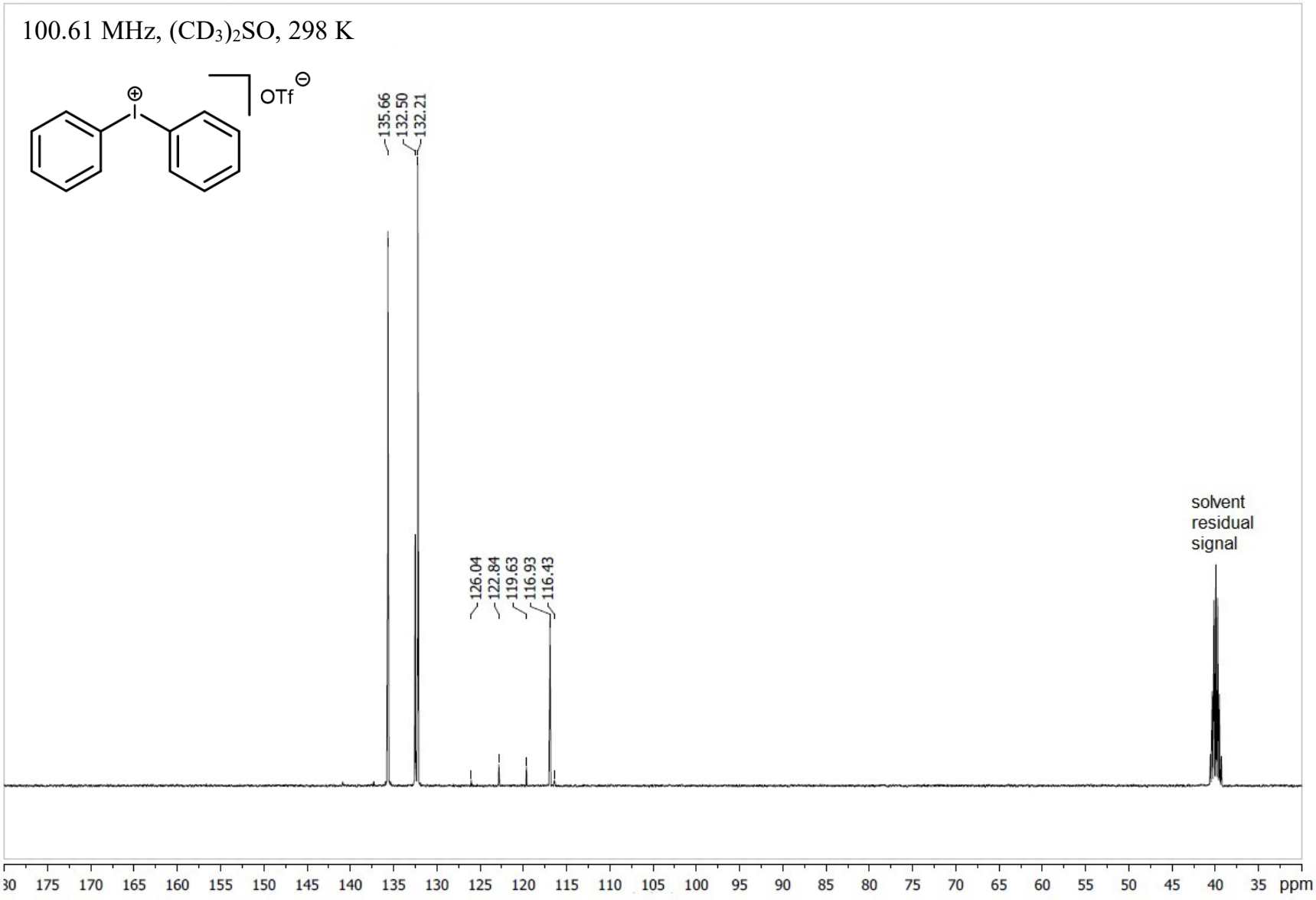

Figure S4. $^{13}C\{^{1}H\}$ NMR spectrum of the **1**^{OTf}.

100.61 MHz, $(CD_3)_2SO$, 298 K

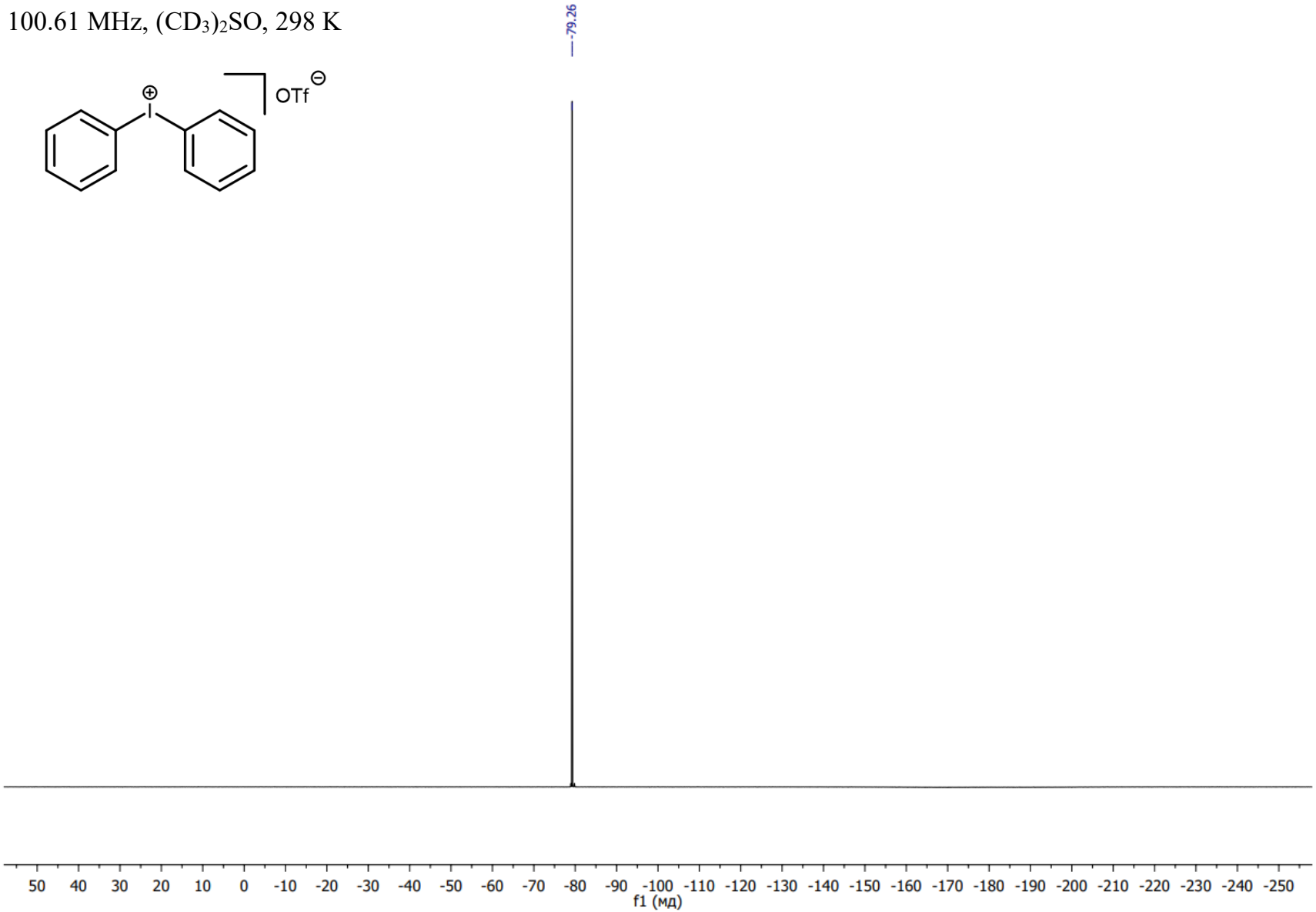

Figure S5. ^{19}F NMR spectrum of the $\mathbf{1}^{OTf}$.

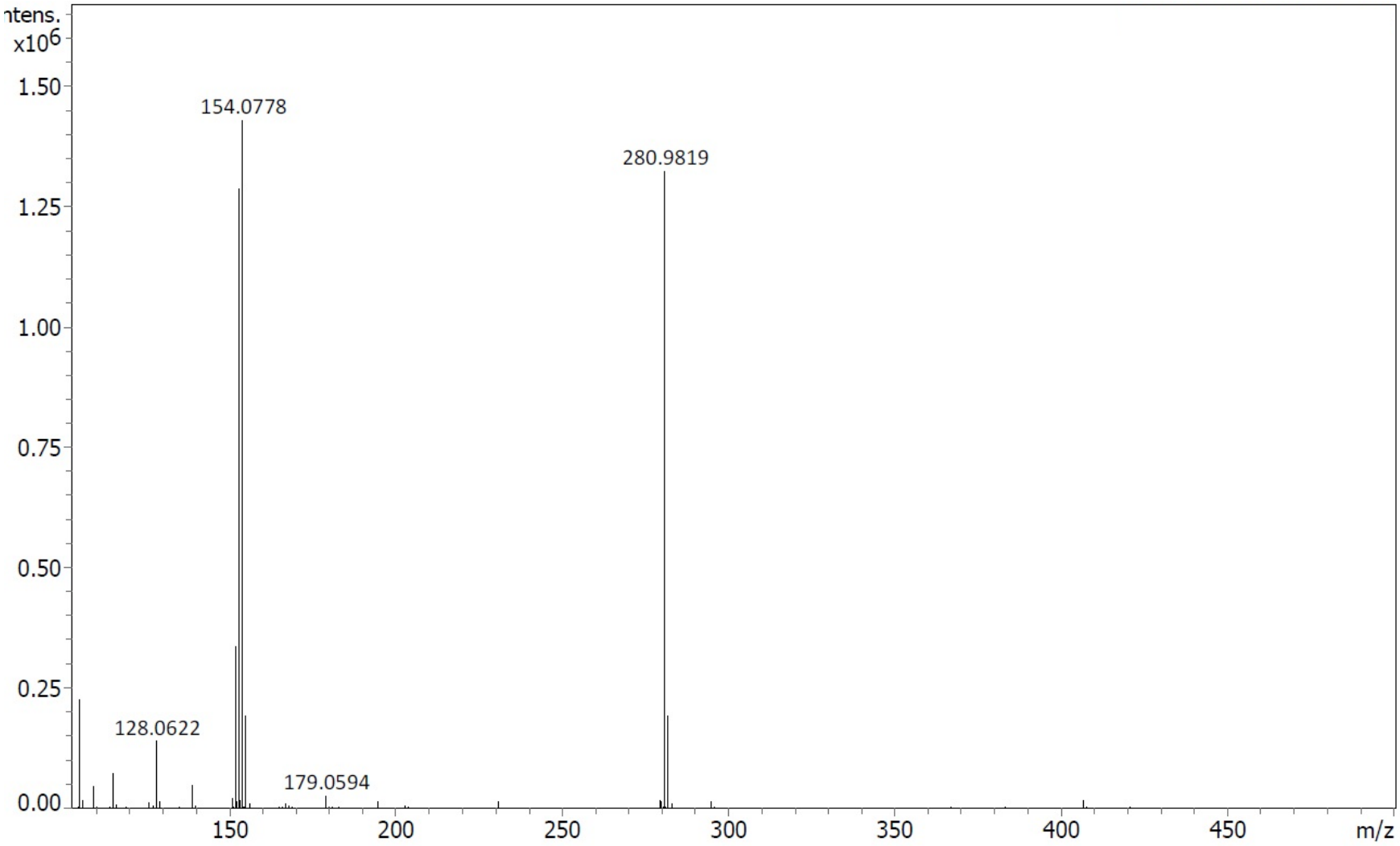

Figure S6. HRES^{+}-MS spectrum of the **1**^{OTf}.

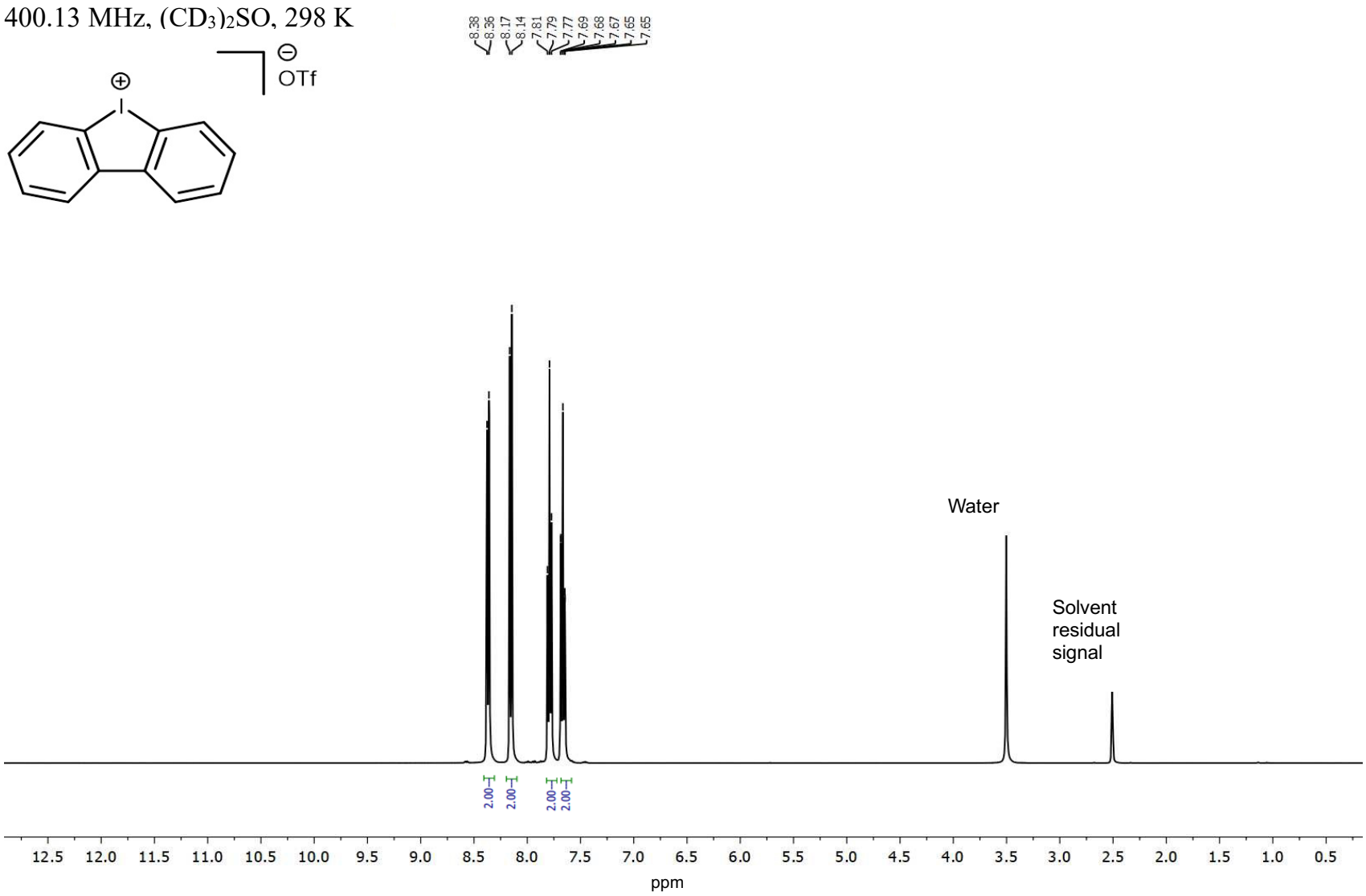

Figure S7. ^{1}H NMR spectrum of **2**^{OTf}.

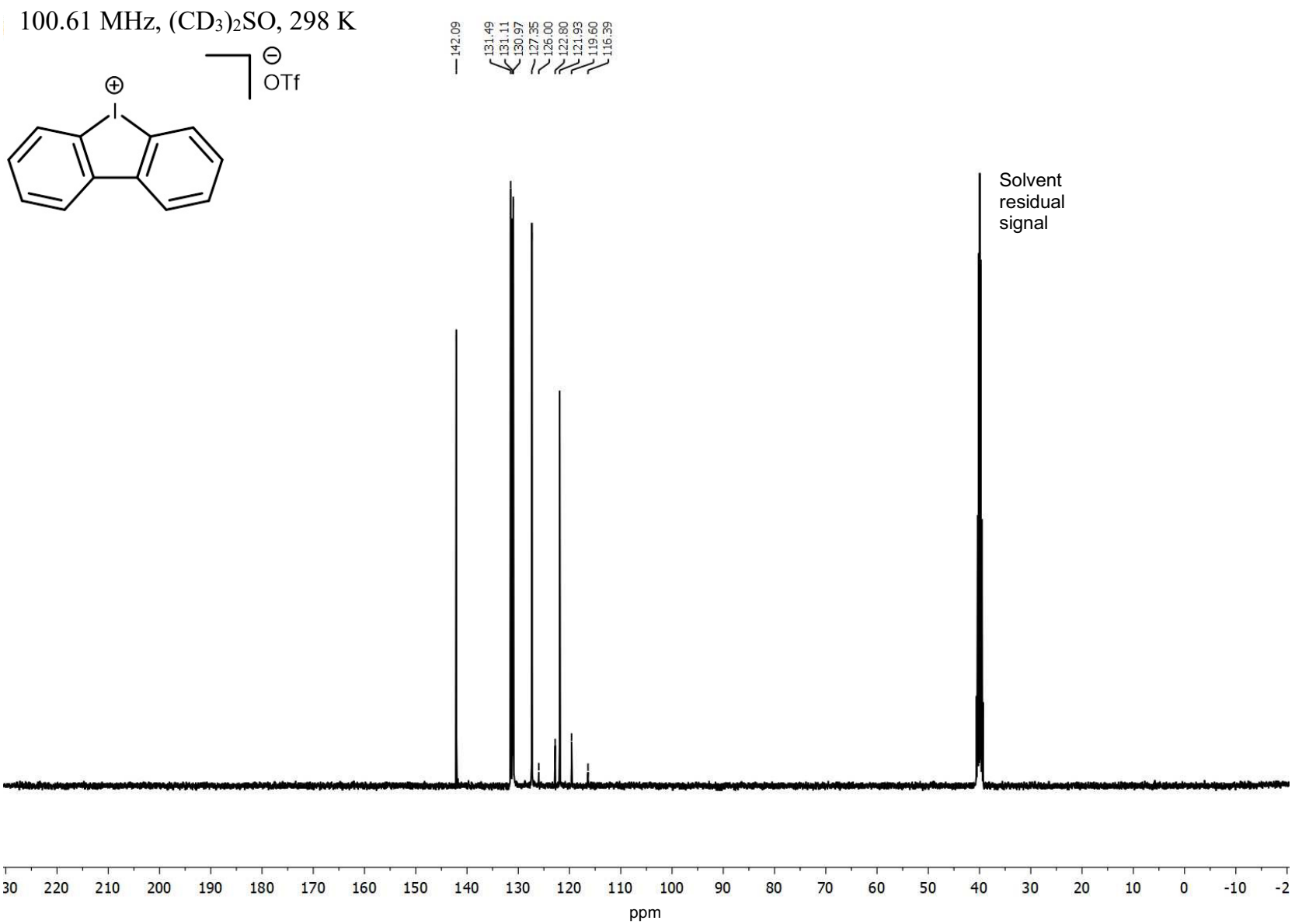

Figure S8. $^{13}C\{^{1}H\}$ NMR spectrum of the **2**^{OTf}.

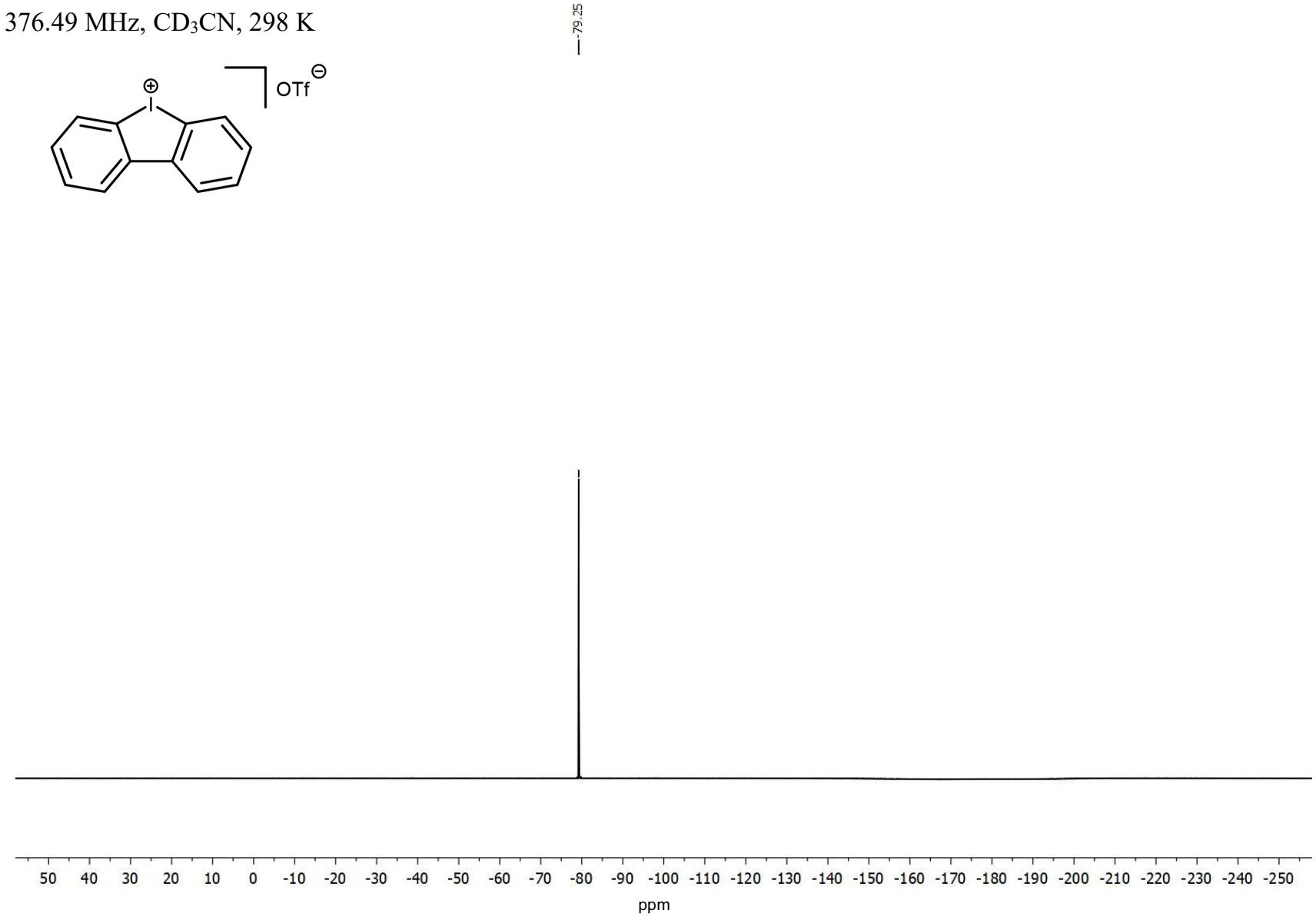

Figure S9. ^{19}F NMR spectrum of the **2**^{OTf}.

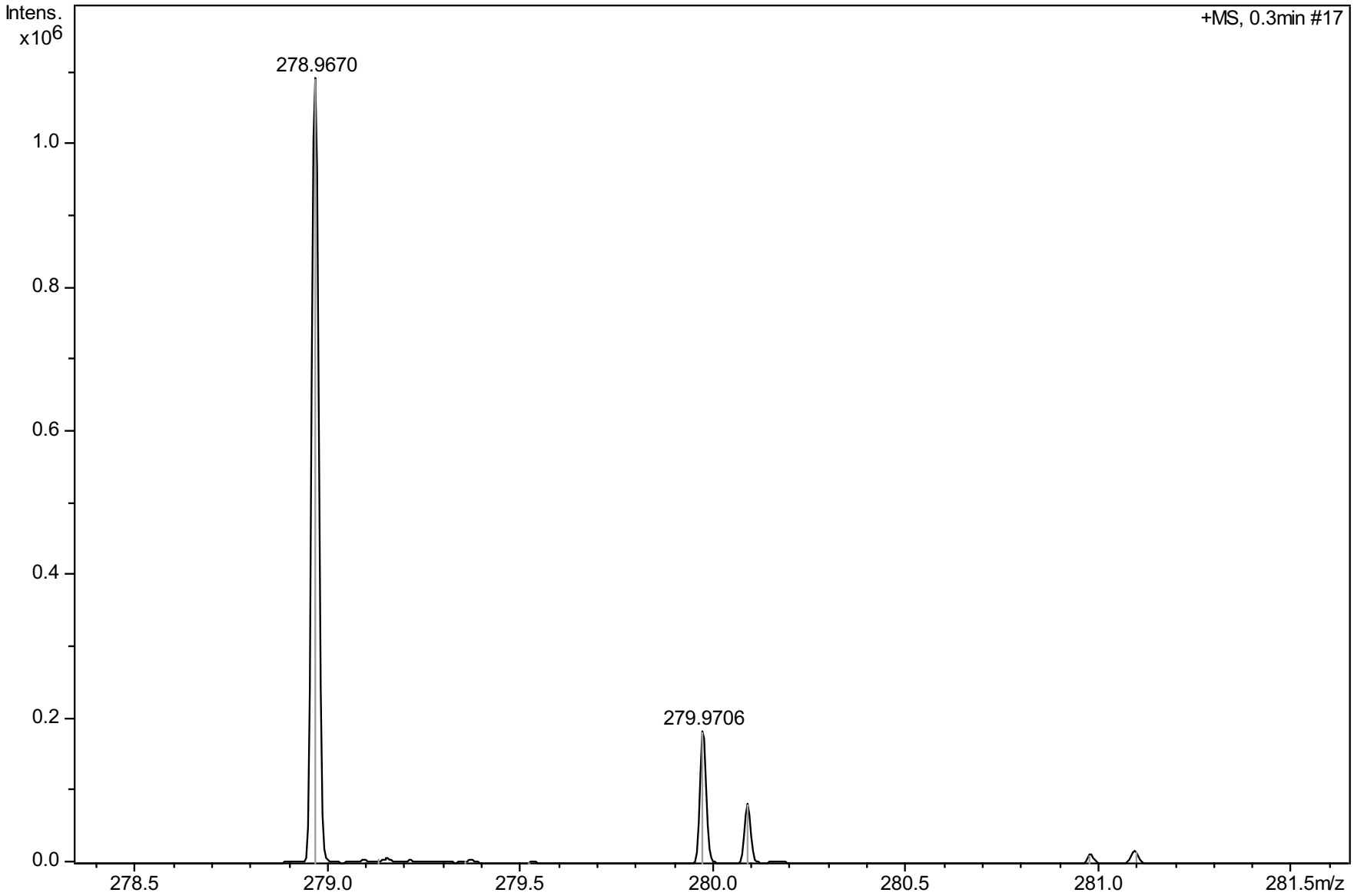

Figure S10. HRES^{+}-MS spectrum of the **2**^{OTf}.

Calculation data

Table S5. Calculated total electronic energies (E, in Hartree), enthalpies (H, in Hartree), Gibbs free energies (G, in Hartree), and entropies (S, cal/mol•K) for optimized equilibrium model structures.

Model structure	E	H	G	S
Methanol				
1$^+$	−473.144237450	−472.971681	−473.019871	101.425
2$^+$	−474.335753748	−474.139961	−474.192883	111.384
18C6	−922.741190214	−922.345039	−922.414328	145.830
1$^+$·18C6	−1395.91484689	−1395.343345	−1395.438290	199.828
1$^+$·18C6·**1**$^+$	−1869.08023905	−1868.332622	−1868.455242	258.076
2$^+$·18C6	−1397.10930217	−1396.514667	−1396.612652	206.225
2$^+$·18C6·**2**$^+$	−1871.47395117	−1870.680486	−1870.807811	267.979
Acetonitrile				
1$^+$	−473.147252794	−472.974707	−473.023674	103.061
2$^+$	−474.338820481	−474.143126	−474.195292	109.793
18C6	−922.728721993	−922.334731	−922.403613	144.974
1$^+$·18C6	−1395.90566093	−1395.334750	−1395.429152	198.684
1$^+$·18C6·**1**$^+$	−1869.07473186	−1868.326635	−1868.443322	245.588
2$^+$·18C6	−1397.10104862	−1396.507161	−1396.604943	205.799
2$^+$·18C6·**2**$^+$	−1871.46746102	−1870.674637	−1870.801292	266.567

Table S6. Crystal data for $\mathbf{1}^{OTf}$·18C6·$\mathbf{1}^{OTf}$.

Identification code	$\mathbf{1}^{OTf}$·18C6·$\mathbf{1}^{OTf}$
Empirical formula	$C_{38}H_{44}F_6I_2O_{12}S_2$
Formula weight	1124.65
Temperature/K	100(2)
Crystal system	triclinic
Space group	P-1
a/Å	9.5421(2)
b/Å	9.8378(2)
c/Å	12.7043(2)
α/°	89.682(2)
β/°	88.449(2)
γ/°	63.993(2)
Volume/Å^3	1071.41(4)
Z	1
ρ_{calc} g/cm^3	1.743
μ/mm^{-1}	13.199
F(000)	560
Crystal size/mm^3	0.07 × 0.05 × 0.03
Radiation	Cu Kα (λ = 1.54184)
2Θ range for data	6.96 to 124.998
Index ranges	-10 ≤ h ≤ 10, -11 ≤ k ≤ 11, -
Reflections collected	11991
Independent reflections	3403 [R_{int} = 0.0714, R_{sigma} =
Data/restraints/parameters	3403/0/265
Goodness-of-fit on F^2	1.083
Final R indexes [I⩾2σ (I)]	R_1 = 0.0533, wR_2 = 0.1390
Final R indexes [all data]	R_1 = 0.0548, wR_2 = 0.1404
Largest diff. peak/hole / e·Å^{-3}	3.15/-1.41
CSD code	2361448

Data Availability Statement

The data supporting this article have been included as part of the Supplementary Information.

Crystallographic data for $\mathbf{1}^{OTf}$·18C6·$\mathbf{1}^{OTf}$ can be obtained free of charge via the Cambridge Crystallographic Database (CCDC 2361448; https://www.ccdc.cam.ac.uk/structures/).

Halogen Bonded Associates of Iodonium Salts with 18-Crown-6: Does Structural Flexibility or Structural Rigidity of the σ-Hole Donor Provide Efficient Substrate Ligation?

Alexandra A. Sysoeva,[1] Alexander S. Novikov,[1,2] Mikhail V. Il'in,[1] and Dmitrii S. Bolotin[1,*]

[1] Institute of Chemistry, Saint Petersburg State University, Universitetskaya Nab. 7/9, Saint Petersburg, 199034, Russian Federation
[2] Peoples' Friendship University of Russia (RUDN University), Miklukho-Maklaya Str. 6, 117198 Moscow, Russian Federation

* Corresponding author E-mail: d.s.bolotin@spbu.ru

Abstract

^{1}H NMR titration of 18-crown-6 with diphenyliodonium triflate and dibenziodolium triflate indicated that the acyclic iodine(III)-containing species has a higher value of the binding constant compared with that of the cyclic analogue. Formation of triple associates diphenyliodonium···18-crown-6···diphenyliodonium was observed in CD_3CN. DFT calculations and QTAIM analysis indicated that the acyclic iodonium salt forms a higher number of interactions with the crown ether compared with the cyclic cation, which results in the formation of triple associates. The formation of dibenziodolium···18-crown-6···dibenziodolium triple associates turned out energetically unfavorable, which agrees with the experimentally obtained data.

Introduction

Diaryliodonium salts play an important role in modern organic chemistry due to their useful applications in synthetic organic chemistry as reactive arylating agents and noncovalent electrophilic organocatalysts.[1] In particular, the iodonium salts effectively catalyze such important transformations as Mannich,[2] Michael,[3] and Groebke–Blackburn–Bienaymé[4-6] reactions, as well as Knoevenagel,[7] Knorr-type, [8] and Schiff condensations,[9] Ritter-type solvolysis,[10, 11] Diels-Alder reaction,[3, 11, 12] living cationic polymerization,[13] and other reactions.[14-16] Such catalytic activity is provided via the availability of a region with

positive electrostatic potential (σ-hole) on the iodine(III) center, which serves as a labile coordination vacancy capable to ligate reaction substrates. A notable catalytic activity of these σ-hole carriers is accompanied with high tolerance to water and oxygen, which positively distinguishes them from metal-containing Lewis acids.[7] These observations may indicate that the replacement of traditional hydrogen bond-donating organocatalysts,[17-20] as well as metal-containing Lewis acids, with iodonium salts can provide the next step in sustainable catalysis.

A series of experimental and theoretical studies indicates that cyclic derivatives of iodonium salts — iodolium derivatives (**Scheme 1**) — have higher catalytic activity and higher Lewis acidity than their acyclic analogues — diaryliodonium salts (**Scheme 1**),[4, 8, 21] which is explained, in particular, by higher binding constants of the former with reaction substrates leading to higher equilibrium concentration of the reactive catalyst···substrate associates.[4] This more profitable binding is provided via fixed location of the *ortho*-hydrogen atoms opposite to the iodine σ-holes leading to the formation of bifurcate halogen- and hydrogen bonding with the ligated reaction substrate.

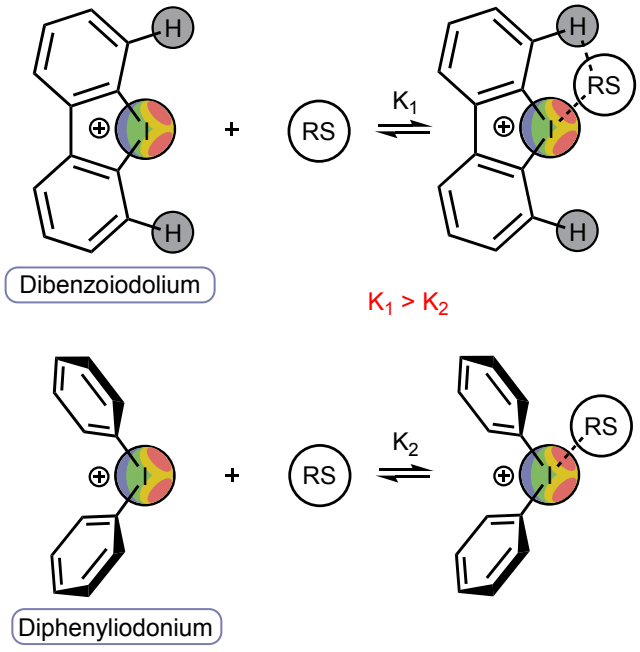

Scheme 1. Reversible association of the iodine(III)-containing cations with a reaction substrate (RS).

In this work, we decided to experimentally and theoretically examine the relative binding constants of dibenziodolium triflate and diphenyliodonium triflate with a bulky nucleophilic agent to check whether the structural flexibility of the acyclic iodonium cation leads to better binding properties compared to the cyclic congener with rigid geometry. A

better understanding of the relative activity of these two types of organocatalysts might help choose a better catalytic system in future research.

Results and Discussion

Experimental study. As model compounds, diphenyliodonium triflate **1**^{OTf} and dibenziodolium triflate **2**^{OTf} have been chosen as model iodine(III)-containing halogen bond donors. 18-Crown-6 has been chosen as a model multidentate nucleophile since its binding with some iodonium cations was studied previously in the solid-state and solution.[22-25] The binding constants have been calculated based on the ^{1}H NMR titration data obtained in acetonitrile-d_3 and methanol-d_4 utilized by us as aprotic and protic solvents, respectively, since both salts are satisfactory soluble in these solvents (**Scheme 2**).

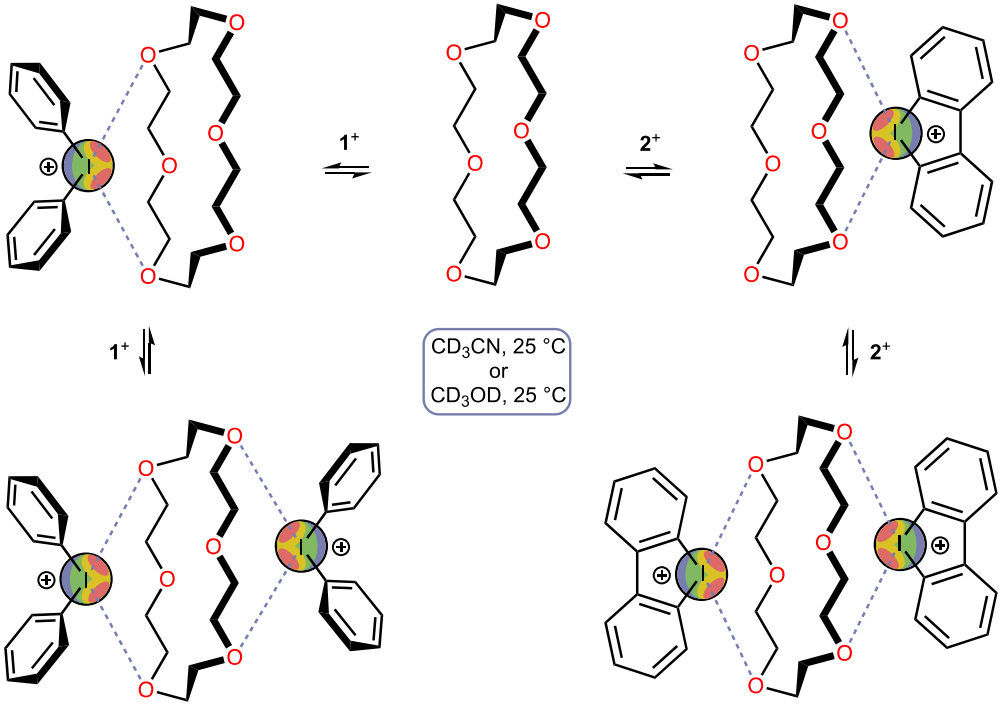

Scheme 2. Simplified representation of a plausible association of the iodine(III)-containing Lewis acids with 18-crown-6 and the conditions utilized for the ^{1}H NMR titration. The counter-ions are omitted for clarity.

Although both cyclic and acyclic iodononium salts previously exhibited excellent titration curves during the study of their binding with a series of simple nucleophiles in protic and aprotic solvents,[4, 5, 7, 8] the titration of 18-crown-6 with **1**^{OTf} or **2**^{OTf} exhibited

some peculiarities. Thus, in CD_3CN, the titration of 18-crown-6 with cyclic $\mathbf{2}^{OTf}$ showed points excellently fitted by the approximation curve (**Figure 1**, top, red line) related to K^{298} = 8.3(4) M^{-1} (1:1 associate), whereas the data obtained for acyclic $\mathbf{1}^{OTf}$ was impossible to fit in the 1:1 or 1:2 approximation models due to counter-directional changes in the chemical shift of 18-crown-6 signal at low and high ratios of the iodonium salt (**Figure 1**, top, blue line). Similar counter-directionality in chemical shift displacement was previously observed by Beer, Langton and co-workers[26] during the titration of multidentate iodine(I)-derived halogen bond donors with chloride, and the authors suggested that this observation is due to a change in the reagent association ratio. Considering this, the obtained in CD_3CN data might indicate the exclusive formation of 1:1 associates of 18-crown-6 with $\mathbf{2}^{OTf}$, and the formation of 1:1 associates 18C6·$\mathbf{1}^{OTf}$ at low concentrations of $\mathbf{1}^{OTf}$ and 1:2 associates at higher values of 18C6:$\mathbf{1}^{OTf}$ ratio. Crystals of the $\mathbf{1}^{OTf}$·18C6·$\mathbf{1}^{OTf}$ associate suitable for XRD study were also prepared via slow evaporation of the mixture of 18-crown-6 and $\mathbf{1}^{OTf}$ (1:2 molar ratio) dissolved in MeCN at room temperature in air (**Figure 2**).

In CD_3OD, titration of 18-crown-6 with $\mathbf{1}^{OTf}$ led to the data being well fitted by the 1:1 host–guest binding model giving K^{298} = 18(3) M^{-1}, whereas the titration with $\mathbf{2}^{OTf}$ was impossible to fit with sufficient accuracy in any association model, which might indicate a low value of the corresponding binding constant. The gradual change in chemical shift in this case should be attributed to the change of media during the increase in the ratio of $\mathbf{2}^{OTf}$.

Taking into account all these experimental observations, it can be concluded that acyclic cation $\mathbf{1}^{OTf}$ exhibits higher affinity to 18-crown-6 in both chosen solvents compared to $\mathbf{2}^{OTf}$, and the binding is more energetically profitable in CD_3CN compared with CD_3OD.

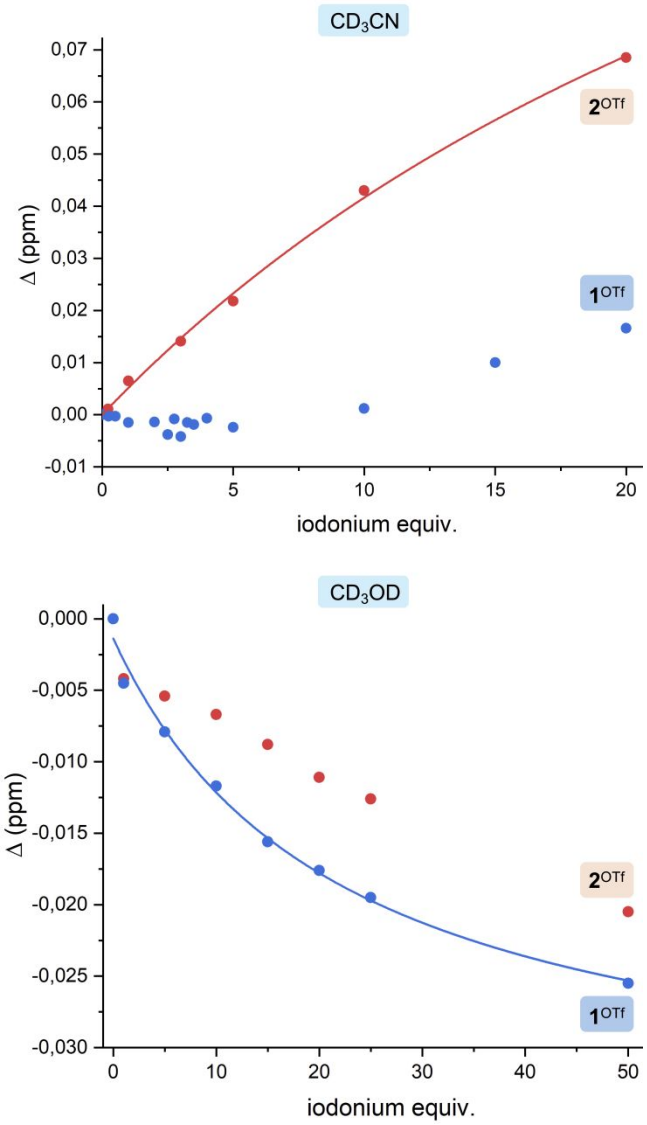

Figure 1. Experimental ^{1}H NMR titration points and calculated curves of mixtures of **1**^{OTf} or **2**^{OTf} with 18-crown-6. The plot represents the shift of the resonance peak of the 18-crown-6. The approximation curves and the corresponding K^{298} values were calculated using Bindfit software using a 1:1 host–guest binding model.

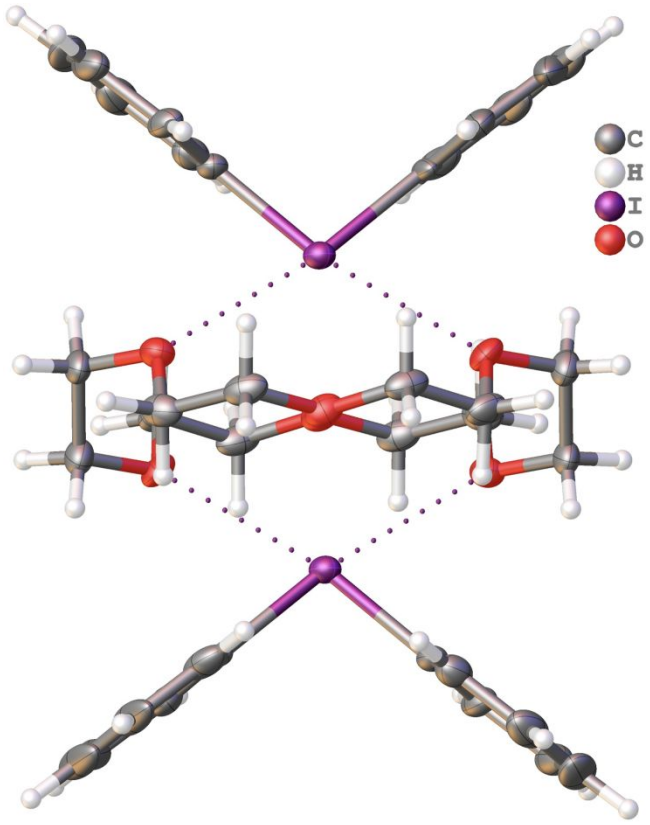

Figure 2. A thermal ellipsoid plot for $\mathbf{1}^{OTf}$·18C6·$\mathbf{1}^{OTf}$. Two triflate anions are omitted for clarity. Thermal ellipsoids are given at the 50% probability level.

Theoretical study. To better understand the reason for the inversion of relative binding constants for acyclic and cyclic iodonium salts relatively to previously published results, the corresponding DFT calculations have been carried out (see Computational Details). In the computational model, the triflate anion was omitted, as most of the effects from the counter-anion are absorbed by solvation correction.[27] The obtained results turned out to be in qualitative agreement with the experimentally obtained data (**Table 1**). In all cases, binding of 18-crown-6 with acyclic $\mathbf{1}^+$ is more energetically favorable than the binding with cyclic $\mathbf{2}^+$. Moreover, in MeCN, formation of 1:1 associate $\mathbf{2}^+$·18C6 has comparable value of the Gibbs free energy with the formation of 1:2 associate $\mathbf{1}^+$·18C6·$\mathbf{1}^+$, which confirms the suggestion made based on the experimental data. In both solvents, the formation of $\mathbf{2}^+$·18C6·$\mathbf{2}^+$ is clearly unfavorable under the studied conditions, which explains good fitting of the experimental plot for 1:1 association in the case of a high concentration of $\mathbf{2}^+$ in MeCN.

Table 1. Calculated values of Gibbs free energies of reaction for model processes $\Delta G = G_{product} - \Sigma G_{reactants}$. Calculated total electronic energies, enthalpies, Gibbs free energies,

and entropies for all optimized equilibrium model structures are given in Supporting Information.

Model association	ΔG, kJ mol^{-1}	
	MeCN	MeOH
1$^+$ + 18C6 → **1**$^+$·18C6	–15.9	–14.3
2$^+$ + 18C6 → **2**$^+$·18C6	–4.9	–10.7
1$^+$ + **1**$^+$ + 18C6 → **1**$^+$·18C6·**1**$^+$	–2.8	–6.0
2$^+$ + **2**$^+$ + 18C6 → **2**$^+$·18C6·**2**$^+$	25.0	7.7

To visualize intermolecular interactions in the optimized equilibrium model structures **1**$^+$·18C6, **2**$^+$·18C6, **1**$^+$·18C6·**1**$^+$, and **2**$^+$·18C6·**2**$^+$, the noncovalent interactions analysis (NCI)[28] was additionally performed for model supramolecular associates (**Figure 2**). The iodonium cations interact with the whole molecule of the crown ether, and it is difficult to definitely identify any dominant type of noncovalent interactions in such chemical systems via this method, particularly in the solution state. In fact, all the contacts I···O could be classified as weak interactions, but a minority of them can be classified as halogen bonds due to their failure to meet geometric criteria. Nevertheless, the NCI analysis indicated that acyclic iodonium cation forms higher number of noncovalent interactions with the crown ether (**Figure 2**, top) than its cyclic analogue (**Figure 2**, bottom), due to the interactions of 18-crown-6 with the π-system of the phenyl rings. Such types of interactions have been theoretically observed by us previously for other onium salts.[29]

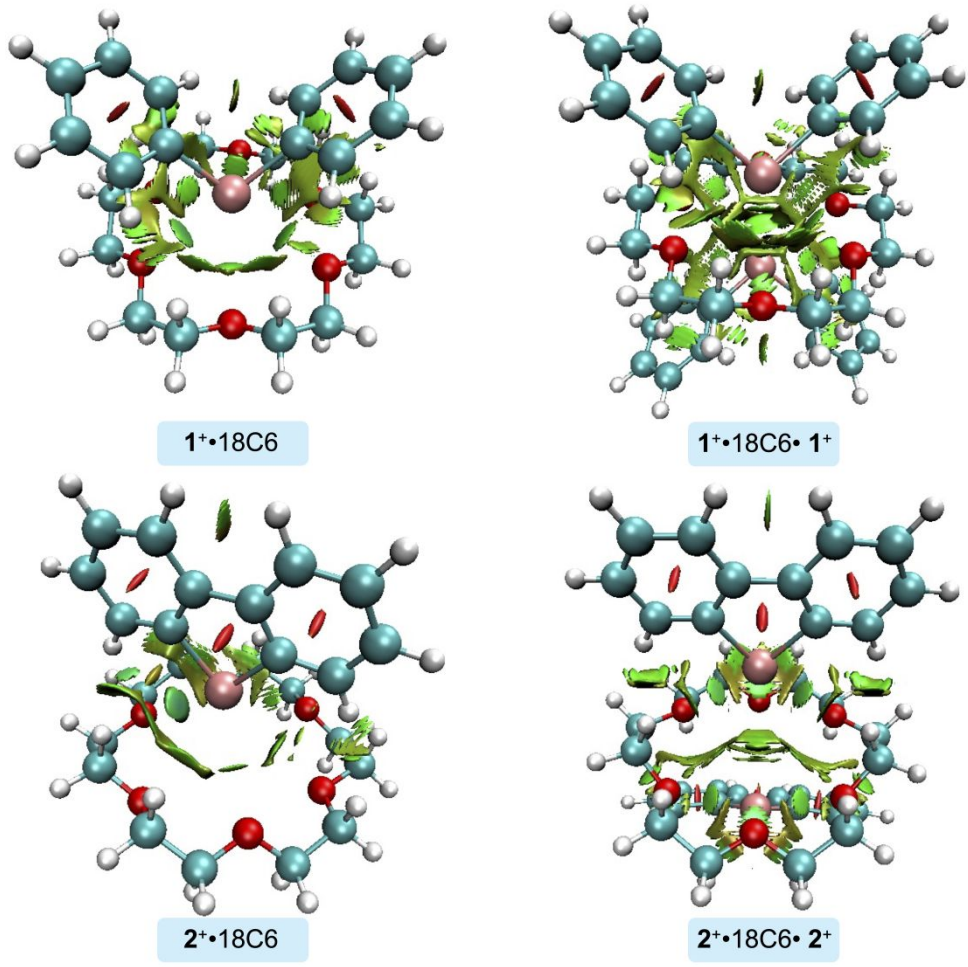

Figure 2. Visualization of intermolecular contacts in calculated structures of the associates **1**$^{+}$·18C6, **2**$^{+}$·18C6, **1**$^{+}$·18C6·**1**$^{+}$, and **2**$^{+}$·18C6·**2**$^{+}$ using NCI analysis technique.

To estimate the relative energy of weak interactions, QTAIM analysis has been performed for model associates **1**$^{+}$·18C6 and **2**$^{+}$·18C6 (**Table 2**). The obtained data indicate that the total estimated energy of all weak interactions between two species in **1**$^{+}$···18C6 equals to 64.3 kJ mol^{-1} those value consists of 24.9 kJ mol^{-1} contribution of two normal halogen bonds, 23.6 kJ mol^{-1} contribution of other four I···O contacts, and additionally 15.7 kJ mol^{-1} from the phenyl···crown interactions. For **2**$^{+}$···18C6, total energy of binding is 52.6 kJ mol^{-1}, which consists of 31.6 kJ mol^{-1} contribution of one hybrid halogen and hydrogen bond and 21.0 kJ mol^{-1} for other five I···O contacts. These data are in full agreement with the experimentally obtained data indicating that **1**$^{+}$ binds the crown ether more efficiently than **2**$^{+}$.

Table 2. Values of the density of all electrons – $\rho(\mathbf{r})$, Laplacian of electron density – $\nabla^2\rho(\mathbf{r})$ and appropriate λ_2 eigenvalues, energy density – H_b, potential energy density – $V(\mathbf{r})$, Lagrangian kinetic energy – $G(\mathbf{r})$, and electron localization function – ELF (a.u.) at the

bond critical points (3, –1), corresponding to selected noncovalent interactions in model supramolecular associates **1**$^{+}$•18C6 and **2**$^{+}$•18C6 (methanol solution), and estimated strength for these weak contacts E_{int} (kJ/mol).

Contact	Bond distance (Å)	$\rho(\mathbf{r})$	$\nabla^2\rho(\mathbf{r})$	λ_2	H_b	$V(\mathbf{r})$	$G(\mathbf{r})$	ELF	$E_{int} \approx -V(\mathbf{r})/2$
1^{+}•18C6									
I···O	3.047	0.015	0.055	–0.015	0.000	–0.011	0.011	0.045	14.4
	3.183	0.011	0.042	–0.011	0.001	–0.008	0.009	0.032	10.5
	3.308	0.010	0.037	–0.010	0.001	–0.007	0.008	0.031	9.2
	3.545	0.007	0.024	–0.007	0.001	–0.004	0.005	0.017	5.3
	3.607	0.006	0.022	–0.006	0.001	–0.004	0.005	0.018	5.3
	3.644	0.005	0.019	–0.005	0.001	–0.003	0.004	0.011	3.9
C_{Ph}···H	2.744	0.007	0.024	–0.007	0.001	–0.004	0.005	0.027	5.3
	2.743	0.007	0.025	–0.007	0.002	–0.003	0.005	0.023	3.9
	2.838	0.007	0.022	–0.007	0.001	–0.003	0.004	0.022	3.9
	2.849	0.006	0.019	–0.006	0.002	–0.002	0.004	0.019	2.6
2^{+}•18C6									
I···O	2.963	0.017	0.066	–0.017	0.001	–0.012	0.013	0.055	15.8
	3.474	0.007	0.028	–0.007	0.001	–0.005	0.006	0.020	6.6
	3.523	0.007	0.026	–0.007	0.001	–0.004	0.005	0.018	5.3
	3.643	0.005	0.019	–0.005	0.001	–0.003	0.004	0.013	3.9
	3.619	0.005	0.020	–0.005	0.001	–0.003	0.004	0.013	3.9
	3.867	0.003	0.012	–0.003	0.001	–0.001	0.002	0.004	1.3
H···O	2.295	0.015	0.049	–0.015	0.000	–0.012	0.012	0.046	15.8

Conclusion

In this work, we have shown that relative ability to bind nucleophilic species of cyclic and acyclic iodonium salts depends on the nature of model nucleophile chosen for the study. The major part of articles dealing with the titration of halogen bond donors typically utilize simple unbulky nucleophilic agents like halides or *C*-, *N*-, or *O*-donors.[4, 21] In these cases, cyclic iodonium salts exhibit higher values of binding constants due to ability to form bifurcate halogen and hydrogen bonding with the Lewis base which is stronger than conventional halogen bonding in the case of acyclic iodonium salts (**Table 2**). Nevertheless, in the case of association with a bulky Lewis base, structural flexibility of acyclic iodonium cations allows them to better associate with the base since the σ-holes of the cation are more accessible for the interaction, whereas the phenyl π-system might provide additional binding of the nucleophilic agent (**Scheme 3**).

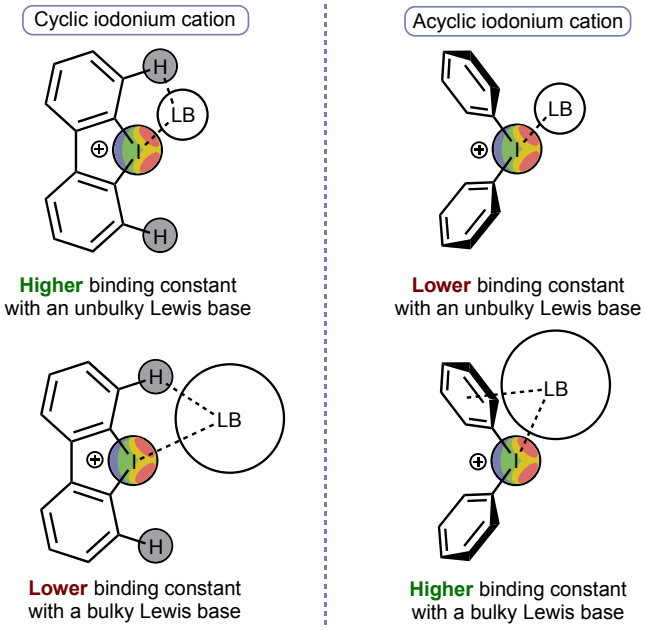

Scheme 3. Binding of cyclic and acyclic iodonium salts with unbulky and bulky Lewis base.

Taking these observations into account, it should be concluded that the utilization of acyclic iodonium salts instead of their cyclic analogues might be a rational choice for the catalysis of organic transformations involving bulky substrates and/or proceeding via bulky transition states.

Experimental Section

Materials and instrumentation. All solvents and reagents were obtained from commercial sources and used as received. The diphenyliodonium and dibenziodolium triflates were synthesized according to published procedure.[4] All syntheses were conducted in air. ^{1}H NMR spectra were measured on a Bruker Avance 400 spectrometer in CD_3CN and CD_3OD at 298 K; the residual solvent signal was used as the internal standard. The electrospray ionization mass-spectra were obtained on a Bruker maXis spectrometer equipped with an electrospray ionization (ESI) source. The instrument was operated in a positive ion mode using an *m*/*z* range 100–1000. The nebulizer gas flow was 1.0 bar and the drying gas flow 4.0 L min^{-1}. For HRESI$^+$, the studied compounds were dissolved in MeOH.

^{1}H NMR titration data. To a series of mixtures of 18-Crown-6 (0.037 M, 50 μL) and diphenyliodonium triflate or dibenziodolium triflate (up to 50-fold excess; see Supporting Information) in NMR tubes, CD_3CN or CD_3OD wasadded to achieve a volume of resulting

solution equal to 500 μL. The 18-Crown-6 signal was used to track the changes in the chemical shift in ^{1}H NMR spectra during variation of the iodonium salt concentration.

Syntheses of the iodonium salts. *Diphenyliodonium triflate (**1**^{OTf}). m*-CPBA (77 %, 1.5 equiv, 6 mmol, 1.348 g) and TfOH (3.0 equiv, 12 mmol, 1.061 mL) were added to a stirred solution of iodobenzene (1.0 equiv, 4 mmol, 0.448 mL) and benzene (1.0 equiv, 4 mmol, 0.355 mL) in dry CH_2Cl_2 (10 mL) and the resulting solution was stirred for 1 h at RT. Then the solvent was evaporated *in vacuo* at RT, and the product was crystallized using Et_2O (10 mL). The obtained heterogeneous solution was stirred for 20 min at RT and then the solid phase was filtered off, washed with Et_2O (10 mL), and dried at 50 °C in air.

White crystalline solid. Yield: 82 % (1.41 g). M.p.: 168–170 °C. δ = 8.28 – 8.26 (m, 4H), 7.67 – 7.63 (m, 2H), 7.55 – 7.51 (m, 4H). ^{13}C{^{1}H} NMR (100.61 MHz, $(CD_3)_2SO$): δ = 135.66, 132.50, 132.21, 116.93 (Ar), 121.23 (q, $^1J_{CF}$ = 322.3 Hz, *C*F$_3$). ^{19}F NMR (376.49 MHz, CD_3CN): δ = –79.26 (s, C*F*$_3$). HRMS (ESI-TOF): *m/z* [M]$^+$ calcd for $C_{12}H_{10}I$: 280.9822; found: 280.9819.

*Dibenziodolium triflate (**2**^{OTf}). m*-CPBA (77 %, 1.5 equiv, 2.96 mmol, 665 mg) and TfOH (3.0 equiv, 5.89 mmol, 0.521 mL) were added to a stirred solution of 2-iodo-1,1'-biphenyl (1.0 equiv, 1.97 mmol, 550 mg) in dry CH_2Cl_2 (5 mL) and stirred for 1 h at RT. Then the solvent was evaporated *in vacuo* at RT, and the product was crystallized using Et_2O (10 mL). The obtained heterogeneous solution was stirred for 20 min at RT and then the solid phase was filtered off, washed with Et_2O (10 mL), and dried at 50 °C in air.

White crystalline solid. Yield: 90 % (760 mg). M.p.: 240–242 °C. ^{1}H NMR (400.13 MHz, $(CD_3)_2SO$): δ = 8.37 (dd, $^3J_{HH}$ = 8.1 Hz, $^4J_{HH}$ = 1.5 Hz, 2H, Ar), 8.15 (d, $^3J_{HH}$ = 8.1 Hz, 2H, Ar), 7.79 (t, $^3J_{HH}$ = 7.8 Hz, 2H, Ar), 7.67 (td, $^3J_{HH}$ = 7.8 Hz, $^4J_{HH}$ = 1.5 Hz, 2H, Ar). ^{13}C{^{1}H} NMR (100.61 MHz, $(CD_3)_2SO$): δ = 142.1, 131.5, 131.1, 131.0, 127.4, 121.9 (Ar), 121.2 (q, $^1J_{CF}$ = 322.3 Hz, *C*F$_3$). ^{19}F NMR (376.49 MHz, CD_3CN): δ = −79.25 (s, C*F*$_3$). HRMS (ESI-TOF): *m/z* [M]$^+$ calcd for $C_{12}H_8I$: 278.9665; found: 278.9670.

Computational details. The full geometry optimization procedure with UFF pre-optimization in Avogadro program package (https://avogadro.cc/) for all model structures was carried out at the DFT level of theory using the hybrid functional ωB97XD[30] (the addition of dispersion correction is *de facto* a standard practice in modern computational chemistry, and it was automatically internally employed in the functional ωB97XD specifically developed for these purposes) with the help of Gaussian-09[31] program package (revision C.01). The iodine is a heavy and relativistic atom and application of special basis sets and pseudopotentials for proper description of the properties of such atoms are highly desirable. By this reason, we used the quasi-relativistic MWB46

pseudopotentials, which described 46 core electrons, and the appropriate contracted basis sets for iodine atoms,[32] while the standard 6-311G* basis sets were used for all other atoms. Note that it is well known from many original articles and benchmark studies[33-36] that triple-zeta quality basis sets (including 6-311G*) are good enough and produce very small basis set superposition errors. No symmetry restrictions were applied during the geometry optimization procedure. The solvent effects were taken into account using the SMD (Solvation Model based on Density) continuum solvation model suggested by Truhlar and coworkers[37] for methanol and acetonitrile as solvents. We used standard default settings for SMD model implemented in Gaussian-09 program package (revision C.01) – atomic radii: SMD-Coulomb, atomic radii for non-electrostatic terms: SMD-CDS, cavity type: VdW (van der Waals surface), cavity algorithm: GePol, solvents: acetonitrile (Eps = 35.688; Eps(inf) = 1.806874) and methanol (Eps = 32.613; Eps(inf) = 1.765709). The Hessian matrices were calculated analytically for all optimized model structures to prove the location of the correct minimum on the potential energy surface (no imaginary frequencies were found in all cases) and to estimate the thermodynamic parameters, the latter being calculated at 298 K and 1 atm. The noncovalent interactions analysis (NCI) have been performed by using the Multiwfn program (version 3.7),[38] and visualized by using the VMD program.[39] The topological analysis of the electron density distribution in model structures within the “atoms in molecules” (QTAIM) method[40] was performed by using the Multiwfn program[38] (version 3.7). The Cartesian atomic coordinates for all model structures are presented in the attached xyz-file, Supporting Information.

Single-crystal XRD study. Single-crystal X-ray diffraction experiment was carried out on Agilent Technologies «SuperNova» diffractometer with monochromated CuKα radiation. Crystals were kept at 100(2) K during data collection. Structure have been solved by the Superflip[41, 42] and the ShelXT[43] structure solution programs using Charge Flipping and Intrinsic Phasing and refined by means of the ShelXL[44] program incorporated in the OLEX2[45] program package. The crystal data and details of structure refinements for $\mathbf{1}^{OTf}$·18C6·$\mathbf{1}^{OTf}$ are shown in **Table S6**. The structures can be obtained free of charge via the Cambridge Crystallographic Database (CCDC 2361448; https://www.ccdc.cam.ac.uk/structures/).

Conflict of interest

There are no conflicts to declare.

Supporting Information

Titration data; Spectra of the iodonium salts; Calculation data; Crystal data for $\mathbf{1}^{OTf}$·18C6·$\mathbf{1}^{OTf}$ (**PDF**)

Optimized model structures (**XYZ**)

Acknowledgements

This work was supported by the Saint Petersburg State University (grant 103922061 — synthetic work) and RUDN University Scientific Projects Grant System (project No 021342-2-000 — DFT calculations). Physicochemical studies were performed at the Center for Magnetic Resonance, and Center for Chemical Analysis and Materials Research (all at Saint Petersburg State University).

Author ORCIDs:

Alexandra A. Sysoeva: 0000-0003-2317-6095

Alexander S. Novikov: 0000-0001-9913-5324

Mikhail V. Il'in: 0000-0003-4234-4779

Dmitrii S. Bolotin: 0000-0002-9612-3050

References

1. X. Peng, A. Rahim, W. Peng, F. Jiang, Z. Gu and S. Wen, *Chem. Rev.*, 2023, **123**, 1364–1416.
2. Y. Zhang, J. Han and Z.-J. Liu, *RSC Adv.*, 2015, **5**, 25485–25488.
3. F. Heinen, D. L. Reinhard, E. Engelage and S. M. Huber, *Angew. Chem. Int. Ed.*, 2021, **60**, 5069–5073.
4. M. V. Il'in, A. A. Sysoeva, A. S. Novikov and D. S. Bolotin, *J. Org. Chem.*, 2022, **87**, 4569–4579.
5. M. V. Il'in, D. A. Polonnikov, A. S. Novikov, A. A. Sysoeva, Y. V. Safinskaya and D. S. Bolotin, *ChemPlusChem*, 2023, **88**, e202300304.
6. D. A. Polonnikov, M. V. Il'in, Y. V. Safinskaya, I. S. Aliyarova, A. S. Novikov and D. S. Bolotin, *Org. Chem. Front.*, 2023, **10**, 169–180.
7. A. A. Sysoeva, M. V. Il'in and D. S. Bolotin, *ChemCatChem*, 2024, DOI: 10.1002/cctc.202301668, e202301668.

8. S. N. Yunusova, A. S. Novikov, N. S. Soldatova, M. A. Vovk and D. S. Bolotin, *RSC Adv.*, 2021, **11**, 4574–4583.
9. A. A. Sysoeva, A. S. Novikov, M. V. Il'in and D. S. Bolotin, *Catal. Sci. Technol.*, 2023, **13**, 3375–3385.
10. D. L. Reinhard, F. Heinen, J. Stoesser, E. Engelage and S. M. Huber, *Helv. Chim. Acta*, 2021, **104**, e2000221.
11. F. Heinen, E. Engelage, A. Dreger, R. Weiss and S. M. Huber, *Angew. Chem. Int. Ed.*, 2018, **57**, 3830–3833.
12. Y. Nishida, T. Suzuki, Y. Takagi, E. Amma, R. Tajima, S. Kuwano and T. Arai, *ChemPlusChem*, 2021, **86**, 741–744.
13. R. Haraguchi, T. Nishikawa, A. Kanazawa and S. Aoshima, *Macromolecules*, 2020, **53**, 4185–4192.
14. Y. Yoshida, T. Fujimura, T. Mino and M. Sakamoto, *Adv. Synth. Catal.*, 2022, **364**, 1091–1098.
15. J. Wolf, F. Huber, N. Erochok, F. Heinen, V. Guerin, C. Y. Legault, S. F. Kirsch and S. M. Huber, *Angew. Chem. Int. Ed.*, 2020, **59**, 16496–16500.
16. M. V. Il'in, Y. V. Safinskaya, D. A. Polonnikov, A. S. Novikov and D. S. Bolotin, *J. Org. Chem.*, 2024, **89**, 2916–2925.
17. X. Han, H. B. Zhou and C. Dong, *Chem. Rec.*, 2016, **16**, 897–906.
18. T. James, M. van Gemmeren and B. List, *Chem. Rev.*, 2015, **115**, 9388–9409.
19. Y. Qin, L. Zhu and S. Luo, *Chem. Rev.*, 2017, **117**, 9433–9520.
20. B. Han, X. H. He, Y. Q. Liu, G. He, C. Peng and J. L. Li, *Chem. Soc. Rev.*, 2021, **50**, 1522–1586.
21. R. J. Mayer, A. R. Ofial, H. Mayr and C. Y. Legault, *J. Am. Chem. Soc.*, 2020, **142**, 5221–5233.
22. M. Ochiai, K. Miyamoto, T. Suefuji, S. Sakamoto, K. Yamaguchi and M. Shiro, *Angew. Chem. Int. Ed.*, 2003, **42**, 2191–2194.
23. M. Ochiai, K. Miyamoto, M. Shiro, T. Ozawa and K. Yamaguchi, *J. Am. Chem. Soc.*, 2003, **125**, 13006–13007.
24. M. Ochiai, K. Miyamoto, T. Suefuji, M. Shiro, S. Sakamoto and K. Yamaguchi, *Tetrahedron*, 2003, **59**, 10153–10158.
25. M. Ochiai, T. Suefuji, K. Miyamoto, N. Tada, S. Goto, M. Shiro, S. Sakamoto and K. Yamaguchi, *J. Am. Chem. Soc.*, 2003, **125**, 769–773.
26. A. Docker, X. Shang, D. Yuan, H. Kuhn, Z. Zhang, J. J. Davis, P. D. Beer and M. J. Langton, *Angew. Chem. Int. Ed.*, 2021, **60**, 19442–19450.

27. P. Erdmann, M. Schmitt, L. M. Sigmund, F. Kramer, F. Breher and L. Greb, *Angew. Chem. Int. Ed.*, 2024, DOI: 10.1002/anie.202403356, e202403356.
28. E. R. Johnson, S. Keinan, P. Mori-Sanchez, J. Contreras-Garcia, A. J. Cohen and W. Yang, *J. Am. Chem. Soc.*, 2010, **132**, 6498–6506.
29. A. S. Novikov and D. S. Bolotin, *Org. Biomol. Chem.*, 2022, **20**, 7632–7639.
30. J. D. Chai and M. Head-Gordon, *Phys. Chem. Chem. Phys.*, 2008, **10**, 6615–6620.
31. M. J. Frisch, G. W. Trucks, H. B. Schlegel, G. E. Scuseria, M. A. Robb, J. R. Cheeseman, G. Scalmani, V. Barone, B. Mennucci, G. A. Petersson, H. Nakatsuji, M. Caricato, X. Li, H. P. Hratchian, A. F. Izmaylov, J. Bloino, G. Zheng, J. L. Sonnenberg, M. Hada, M. Ehara, K. Toyota, R. Fukuda, J. Hasegawa, M. Ishida, T. Nakajima, Y. Honda, O. Kitao, H. Nakai, T. Vreven, J. J. A. Montgomery, J. E. Peralta, F. Ogliaro, M. Bearpark, J. J. Heyd, E. Brothers, K. N. Kudin, V. N. Staroverov, T. Keith, R. Kobayashi, J. Normand, K. Raghavachari, A. Rendell, J. C. Burant, S. S. Iyengar, J. Tomasi, M. Cossi, N. Rega, J. M. Millam, M. Klene, J. E. Knox, J. B. Cross, V. Bakken, C. Adamo, J. Jaramillo, R. Gomperts, R. E. Stratmann, O. Yazyev, A. J. Austin, R. Cammi, C. Pomelli, J. W. Ochterski, R. L. Martin, K. Morokuma, V. G. Zakrzewski, G. A. Voth, P. Salvador, J. J. Dannenberg, S. Dapprich, A. D. Daniels, O. Farkas, J. B. Foresman, J. V. Ortiz, J. Cioslowski and D. J. Fox, *Gaussian 09, Revision C.01*, 2010.
32. A. Bergner, M. Dolg, W. Küchle, H. Stoll and H. Preuß, *Mol. Phys.*, 1993, **80**, 1431–1441.
33. B. Paizs and S. Suhai, *J. Comput. Chem.*, 1998, **19**, 575–584.
34. A. Vidal Vidal, L. C. de Vicente Poutas, O. Nieto Faza and C. S. Lopez, *Molecules*, 2019, **24**, 3810.
35. M. Gray, P. E. Bowling and J. M. Herbert, *J. Chem .Theory Comput.*, 2022, **18**, 6742–6756.
36. R. Crespo-Otero, L. A. Montero, W. D. Stohrer and J. M. Garcia de la Vega, *J. Chem. Phys.*, 2005, **123**, 134107.
37. A. V. Marenich, C. J. Cramer and D. G. Truhlar, *J. Phys. Chem. B*, 2009, **113**, 6378–6396.
38. T. Lu and F. Chen, *J. Comput. Chem.*, 2012, **33**, 580–592.
39. W. Humphrey, A. Dalke and K. Schulten, *J. Mol. Graph.*, 1996, **14**, 33–38.
40. R. F. W. Bader, *Chem. Rev.*, 1991, **91**, 893–928.
41. L. Palatinus and G. Chapuis, *J. Appl. Crystallogr.*, 2007, **40**, 786–790.

42. L. Palatinus, S. J. Prathapa and S. van Smaalen, *J. Appl. Crystallogr.*, 2012, **45**, 575–580.
43. G. M. Sheldrick, *Acta Crystallogr.*, 2015, **A71**, 3–8.
44. G. M. Sheldrick, *Acta Crystallogr.*, 2015, **C71**, 3–8.
45. O. V. Dolomanov, L. J. Bourhis, R. J. Gildea, J. A. K. Howard and H. Puschmann, *J. Appl. Crystallogr.*, 2009, **42**, 339–341.